

NASA Contractor Report 3051

NASA
CR
3051
c.1

LOAN COPY: RETURN
AFWL TECHNICAL LIBRARY
KIRTLAND AFB, N.M.

0061791



TECH LIBRARY KAFB, NM

Studies of Convection in a Solidifying System With Surface Tension at Reduced Gravity

Basil N. Antar and Frank G. Collins

CONTRACT NAS8-32484
SEPTEMBER 1978

NASA



NASA Contractor Report 3051

Studies of Convection
in a Solidifying System With
Surface Tension at Reduced Gravity

Basil N. Antar and Frank G. Collins
The University of Tennessee Space Institute
Tullahoma, Tennessee

Prepared for
George C. Marshall Space Flight Center
under Contract NAS8-32484

NASA

National Aeronautics
and Space Administration

**Scientific and Technical
Information Office**

1978

FOREWORD

The research reported herein was supported by NASA contract NAS8-32484. Dr. George H. Fichtl and Mr. Charles Schafer of the Atmospheric Sciences Division, Space Sciences Laboratory, Marshall Space Flight Center, were the scientific monitors; and support was provided by the Office of Applications, NASA Headquarters.

TABLE OF CONTENTS

	<u>Page</u>
I INTRODUCTION	1
II MATHEMATICAL FORMULATION	4
III NON-DIMENSIONAL PARAMETERS	25
IV DISCUSSION	30
V CONCLUSIONS	35
References	36
Figures	38
Tables	51
Appendix I	57
Appendix II	60
Appendix III	61

1. Introduction

One of the principal objectives in the future utilization of orbital laboratories and stations is the production of materials in space. This type of material production is referred to as space processing. One of the primary constituents of most production processes involves the solidification of materials. The broad objective of the present report is to investigate the solidification process in a low gravity environment, while the specific task is to look at the stability of the solid-liquid interface under the same conditions. The meaning of the term stability as used here will be discussed more fully later on in the report.

The problem of material solidification in general has attracted researchers for many decades due to both its importance to industry from the practical point of view and its mathematical difficulty from the theoretical point of view. The analytical solidification problem is commonly known as the "Stefan Problem" in honor of Jakob Stefan (1889), who first formulated it. At the present time, solutions to various aspects of the problem exist under different boundary conditions, such as to make it of practical use for industrial applications. For recent reviews of such solutions the reader is referred to the books by Rubinstein (1971) and Ockendon and Hodgkins (1975). Also, the not-so-recent review articles by Boley (1969) and Muehlbauer and Sunderland (1965) are informative. However, the problem in its entirety is far from solved, as is revealed from a scan of the recent literature which, incidentally, also shows the continued interest in the problem.

The mathematical difficulty of the problem is manifested in the fact that although the governing equations are linear, the boundary conditions are strongly non-linear, with the added difficulty that the boundaries are not stationary. Due to this second complication, almost all of the solutions to the problem are time dependent with only very few exceptions where it is steady.

Careful inspection of the problem reveals that the formulation of the problem is not at all altered when the surrounding environment is at reduced gravity. Hence, all of the mathematical difficulties alluded to earlier are present under the new conditions. However, instead of tackling the full-blown problem for the present report and thus adding relatively little new information, it was decided to look at one aspect of the problem which might be of relevance to space processing. This aspect involves the deformation of the solid-liquid interface from its original form during a solidification process in a reduced gravity environment.

The problem just defined above is not unique to space processing, and there exist quite a few applications for ground base work. If the solidifying material is composed of a binary alloy, for example, it has been shown first by Mullins and Sekerka (1964) and later by Wolkind and Segel (1970) that the solid-liquid interface could deviate from its original planar configuration for both finite and infinitesimal disturbances. On the other hand, if the solidification process is allowed to proceed from the upper boundary of the liquid, instabilities of the Benard type might contribute to the deformation of the phase boundary. Such a problem has been investigated by many workers, some of whom are Turcotte (1974), Schubert et al. (1975), and Busse

and Schubert (1971), where the application was to mantle convection. Also, the same type of instabilities might set in during a melting process if the melting is from below, as is shown analytically by Sparrow et al. (1977) and later verified experimentally also by Sparrow et al. (1978).

In the present report the stability of the solid-liquid interface of a pure metal will be studied during a solidification process in which the liquid surface is free. Two such problems will be considered, one in which the phase boundary is stationary and another in which it is propagating at a constant speed. Note that the added complication due to the solidification of a mixture or a binary alloy is avoided here since it will not greatly enhance the basic understanding of the problem. Since the problem will be analyzed in a zero gravity environment, buoyancy effects do not contribute to the problem, thus leaving only the influence of a variable surface tension to be investigated. Seki et al. (1977) have studied the influence of surface tension coupled with buoyancy effects on the stability of the phase boundary. Their work, however, relates to a stationary phase boundary. Chang and Wilcox (1976), on the other hand, considered the effects of surface tension in a floating zone melting process. However, their analysis was not of the stability type but rather numerical in which the solidification process does not enter.

In the next few sections of this report the problem to be studied will be defined and the equations will be set up with the appropriate boundary conditions. Then the problem will be solved and the results tabulated and discussed. In the final section these results will be discussed as they apply to real working materials such as some pure metals whose use is anticipated in space processing applications.

2. Mathematical Formulation

The complete analysis of the shape of the solid-liquid interface in a general solidification process is extremely complicated, which ultimately might require a complicated numerical solution and thus is beyond the scope of the present report. Alternatively, it is possible to study the stability of the interface for a simple geometrical configuration. By stability of the interface the question is asked: given an original shape of the interface, say, planar, or any other configuration, under what conditions will the shape remain unaltered during the various stages of the solidification process? This is a typical example of a classical hydrodynamic stability problem in which it is determined whether the interface geometry will change if a slight disturbance is imposed on the original configuration. The evolution of this disturbance with time will then determine the fate of the original configuration. If the disturbance decays with time, then the original configuration is said to be stable with respect to the disturbance, and it is unstable otherwise. If the disturbance is infinitesimal, then the stability analysis is called linear, and if it is finite then the analysis is nonlinear. In the present report, only linear stability analysis will be performed.

Since most stability analyses are performed with respect to time, it is imperative that an original state is found which is either independent of, or at most periodic with, time. As discussed in the introduction, in a solidification process the solution is almost always a nonperiodic function of time. For the present study two solutions for the mean state were found which are independent of time,

both of which are analyzed here. The first configuration which is shown in Figure 1 constitutes a fluid and a solid layer which are in equilibrium and hence the liquid-solid interface is planar and stationary. Although such a configuration is not strictly a solidification process it is nevertheless used for illustrative purposes and further to unravel the main difficulties associated with the problem. The second configuration constitutes a continuous solidification process in which the interface boundary is moving at a constant rate. With a simple transformation it will be shown that a steady state solution exists for this process, thus facilitating a manageable linear stability analysis. This second example is closer to a real solidification process and thus is a more realistic example than the first.

Since the present stability analyses are linear, a direct answer to the stability of the interface cannot be obtained. The stability or the instability of the interface will be considered as a consequence of the stability or instability of the fluid. Thus, if the analysis reveals the liquid to be unstable to infinitesimal disturbances, it is then assumed that convection of some sort will set in the liquid in such a way as to disturb the original shape of the interface and probably deform it, as shown schematically in Figure 2. If the fluid is found to be stable, on the other hand, it will be assumed that any initial deformation of the interface will be evened out and the interface will retain its original configuration.

2.1 Steady State Solidification Process

A. The Mean State Solution

It can be formally proven, and will be shown below, that if the upper surface of a melt layer which is on top of a solid layer whose

surfaces are kept at a constant but different temperature each, then part of the melt will solidify until the solid-liquid interface reaches an equilibrium position. This equilibrium position of the solid-liquid interface is a function of both temperatures and the solidification temperature only. This is one of the basic and simple steady state solutions to the Stefan problem [Rubinstein (1971)]. As a first example, the stability of this solution will be studied where a sketch of the problem is provided in Figure 1.

Consider two finite depth layers, one of melt and another of solid, which are infinite in the horizontal direction, where the temperature distribution in both the liquid and solid is denoted by T_l and T_s , respectively. Since there is no convection in the mean state, the energy equations for a steady state are given by

$$\frac{d^2 T_{0s}^*}{dz^{*2}} = 0 \quad ; \quad \frac{d^2 T_{0l}^*}{dz^{*2}} = 0 \quad , \quad (1)$$

with the temperature at the top of the liquid layer given by

$T_{0l}^*(d) = T_2^*$ and the temperature at the bottom of the solid is given by $T_{0s}^*(0) = T_1^*$. In here the asterisk denotes dimensional quantities.

However, since we are considering a solidification process, the energy balance and conservation of mass considerations at the solid-liquid interface imposes the following three additional conditions:

$$\left. \begin{aligned} T_{0s}^* &= T_{0l}^* = T_m^* \\ k_s \frac{dT_{0s}^*}{dz^*} &= k_l \frac{dT_{0l}^*}{dz^*} \end{aligned} \right\} z^* = S \quad (2)$$

where k_s and k_l are the thermal conductivities of the solid and liquid, respectively. T_m^* is the solidification temperature and S is the equilibrium position of the interface.

A solution to equation (1) with all the boundary conditions is given by

$$T_{os} = T_1 + (K T_2 - T_1) z \quad , \quad (3)$$

$$T_{ol} = T_1/k + (T_2 - T_1/k) z \quad ,$$

where

$$T_o = \frac{T_o^* - T_m^*}{T_2^* - T_1^*} \quad ; \quad K = \frac{k_l}{k_s} \quad \& \quad z = z^*/d \quad .$$

The equilibrium position of the interface is uniquely determined by this solution to be

$$\beta = \frac{T_1}{T_1 - K T_2} \quad ,$$

where

$$\beta = S/d \quad . \quad (4)$$

The solution given by (3) is identical to that obtained by Rubinstein (1971) for the time dependent problem in the limit as $\text{time} \rightarrow \infty$. Furthermore, the above solution is no more than the steady conduction solution for the fluid and solid layers with a linear temperature distribution in each.

B. Linear Stability Analysis

In order to investigate whether the interface boundary can withstand a slight perturbation, a linear stability analysis was performed on the mean state solutions (3) and the boundary conditions. The analysis was carried out along lines which are similar to what is commonly done in hydrodynamic stability analyses. The field variables are first decomposed into a mean and a perturbation in the form

$$\begin{aligned} T &= \bar{T}_0 + T' , \\ \vec{u} &= \vec{u}_0 + \vec{u}' , \end{aligned} \quad (5)$$

where T is the temperature field and \vec{u} is the velocity vector. \vec{u}_0 in the present case is zero since it is assumed that there is no convective motion in the mean state. These functions are then substituted into the momentum and energy equations and the mean state is subtracted out. Since we are considering only a linear stability analysis, the remaining equations for the perturbation functions are then linearized. Furthermore, these equations are then manipulated to eliminate the pressure term resulting in the following equations:

$$\left(\frac{\partial}{\partial t} - \frac{\nu}{\kappa_2} \nabla^2 \right) \nabla^2 w' = 0 , \quad (6)$$

$$\left(\frac{\partial}{\partial t} - \nabla^2 \right) T_1' = -w' \frac{dT_{01}}{dz} , \quad (7)$$

$$\left(\frac{\partial}{\partial t} - \frac{\kappa_2}{\kappa_1} \nabla^2 \right) T_s' = 0 . \quad (8)$$

Use has been made in the above equations of the mass conservation equation. In these equations ν is the kinematic viscosity of the liquid, κ_ℓ and κ_s are the thermal diffusivities of the liquid and solid, respectively, and w' is the z component of the velocity vector, and $\frac{dT_{0\ell}}{dz}$ is the temperature gradient of the mean state in the liquid which is a constant in this case. The independent variables in equations (6)-(8) have been made dimensionless in the following way:

$$\begin{aligned}
 (x, y, z) &= (x^*/d, y^*/d, z^*/d) , \\
 t &= t^* \kappa_\ell / d^2 , \\
 w' &= w^{*'} d / \kappa_\ell , \\
 T' &= T^{*'} / (T_2^* - T_m^*) ,
 \end{aligned}
 \tag{9}$$

and

$$\nabla^2 = \frac{\partial^2}{\partial x^2} + \frac{\partial^2}{\partial y^2} + \frac{\partial^2}{\partial z^2} ,$$

where again the asterisk indicates dimensional quantities.

The set (6)-(8) constitutes a linear partial differential system for the perturbation variables w' , T'_s and T'_ℓ . A solution to this set is sought for appropriate boundary conditions which are obtained in the following way. At the lower surface of the solid it is assumed that the temperature perturbation is zero, i.e.,

$$T_\ell^{*'}(0) = 0
 \tag{10}$$

At the top of the surface of the liquid we require the velocity perturbation to be also zero, i.e.,

$$w^{*'}(d+S) = 0
 \tag{11}$$

Also, a radiation condition is imposed on the upper surface of the liquid in the form

$$k_l \frac{\partial T_l^*}{\partial z^*} = -q T_l^* \quad @ \quad z = S + d, \quad (12)$$

where q represents the rate of change with temperature of the rate of loss of heat per unit area from the upper surface to its upper environment. Note if $q \rightarrow \infty$ we approach a conducting boundary condition, while if $q \rightarrow 0$ we approach an insulating boundary condition. A comprehensive discussion of this boundary condition is provided by Pearson (1958). Another condition to be imposed on the upper surface of the liquid layer is that of the balance of the tangential forces on that surface, which is given by Levich and Krylov (1969):

$$\left(\frac{\partial^2}{\partial x^{*2}} + \frac{\partial^2}{\partial y^{*2}} \right) \sigma = \mu \left(\frac{\partial^2}{\partial x^{*2}} + \frac{\partial^2}{\partial y^{*2}} - \frac{\partial^2}{\partial z^{*2}} \right) \omega^* ,$$

where σ and μ are the surface tension and dynamic viscosity of the fluid. Now, since the surface tension is known to be a strong function of temperature, the above condition will be valid only if the temperature of the upper surface is not constant. If instabilities will set in the fluid, the temperature distribution will not be constant on the surface and the surface tension force will play a major role in the stability analysis. For the purpose of the present report it will be assumed that the surface tension is a linear function of temperature in the form

$$\sigma = \sigma_0 + b T^* ,$$

where $b = \frac{\partial \sigma}{\partial T^*_{0l}}$ and σ_0 is a constant. With this approximation the condition for the balance of the tangential forces may be rewritten as:

$$b \left(\frac{\partial^2}{\partial x^{*2}} + \frac{\partial^2}{\partial y^{*2}} \right) T^{*'} = \mu \left(\frac{\partial^2}{\partial x^{*2}} + \frac{\partial^2}{\partial y^{*2}} - \frac{\partial^2}{\partial z^{*2}} \right) w^{*'} \quad @ z = S + d. \quad (13)$$

There remains the boundary conditions at the interface to be satisfied. The first is the requirement that the temperature at the interface regardless of the position of the interface remains the solidification temperature leading to

$$T_s^{*'} = T_l^{*'} = 0 \quad @ z = S. \quad (14)$$

Here it is assumed that the perturbed position of the interface to a first order of approximation is the same as its unperturbed position. Also, at this position, where the solid boundary acts as a wall, the no-slip conditions are imposed and take the form

$$\frac{\partial w^{*'}}{\partial z^*} = 0 \quad @ z = S, \quad (15)$$

while the linearized form of the energy balance at the interface leads to

$$k_s \frac{\partial T_s^{*'}}{\partial z^*} - k_l \frac{\partial T_l^{*'}}{\partial z^*} = -\rho_s L w^{*'}, \quad @ z = S, \quad (16)$$

where ρ_s is the density of the solid and L is the latent heat of fusion. Condition (16) is not intuitively obvious and is rigorously derived in Appendix 1 for the present case and for the subsequent case also.

The linear system of equations (6)-(7) together with the separable linear boundary conditions (10)-(16) admit solutions through the

separation of variables method. To obtain such a solution the perturbation variables must take the following functional form:

$$[w', T_1', T_2'] = [v(z), \theta_1(z), \theta_2(z)] \cos \alpha x \exp(a_0 t) . \quad (17)$$

Note that only a two-dimensional form of the perturbation function is considered, where it is hoped that the analysis is not affected in a major way.

Substituting (17) into (6)-(7) leads to the following system of ordinary differential equations for the perturbation functions

$$[a_0 - P_r (D^2 - \alpha^2)][a_0 - (D^2 - \alpha^2)](D^2 - \alpha^2)\theta_1 = 0 , \quad (18)$$

$$[a_0 - \Delta (D^2 - \alpha^2)]\theta_2 = 0 , \quad (19)$$

where

$$D = \frac{d}{dz} \quad ; \quad \Delta = \kappa_s / \kappa_e \quad ; \quad P_r = \eta / \kappa_e$$

$$a_0 = a_{0r} + i a_{0i}$$

The question of stability or instability can be settled by determining the value of a_0 . Specifically, only the sign of $\text{Re}(a_0)$ is needed since if $\text{Re}(a_0)$ is negative, zero or positive then the system is stable, neutral or unstable, respectively. To even determine the sign of $\text{Re}(a_0)$ is quite tedious and instead the principle of exchange of stability is invoked here. This principle implies that if $\text{Re}(a_0) = 0$ then $\text{Im}(a_0) = 0$ and if this is true, then it is possible to set $a_0 = 0$ in order to determine the neutral stability criteria. Adopting this principle reduces the system of equations to the following:

$$(\mathcal{D}^2 - \alpha^2)^3 \theta_1 = 0 \quad (20)$$

$$(\mathcal{D}^2 - \alpha^2) \theta_5 = 0 \quad (21)$$

while the boundary conditions will take the following form:

$$\mathcal{D} \theta_1(1) + B \theta_1(1) = 0$$

$$(\mathcal{D}^2 - \alpha^2) \theta_1(1) = 0$$

$$(\mathcal{D}^4 - \alpha^4) \theta_1(1) - M \alpha^2 \theta_1(1) = 0$$

$$\theta_1(0) = 0$$

$$\theta_5(0) = 0$$

$$\mathcal{D}(\mathcal{D}^2 - \alpha^2) \theta_1(0) = 0$$

$$\mathcal{D} \theta_5(0) = K \mathcal{D} \theta_1(0) - \frac{P \Lambda}{\Delta T} (\mathcal{D}^2 - \alpha^2) \theta_1(0)$$

$$\theta_5(-\beta) = 0$$

(22)

where

$$B = qd/k_1$$

$$M = (\partial \sigma / \partial T) (\partial T_{01} / \partial z) \frac{d^2}{k_1 \mu}$$

$$\gamma = \partial T_{01} / \partial z \quad ; \quad P = \rho_0 / \rho_s$$

$$\Lambda = \frac{L}{c_{p_s} (T_2 - T_1)}$$

In the above boundary conditions the origin has been shifted to the interface boundary.

The solutions to equations (20) and (21) may be written immediately in the form

$$\begin{aligned} \theta_1(z) = & (A_1 + z A_3 + z^2 A_5) \cosh \alpha z \\ & + (A_2 + z A_4 + z^2 A_6) \sinh \alpha z \end{aligned} \quad (23)$$

$$\theta_5(z) = A_7 \cosh \alpha z + A_8 \sinh \alpha z \quad (24)$$

Satisfying the boundary conditions for the perturbation temperature in the solid leads to

$$A_7 = A_8 = 0,$$

and thus

$$\theta_5 \equiv 0. \quad (25)$$

However, A_1 through A_6 may be determined from the conditions on the perturbation temperature in the liquid. Since we are looking for neutral stability curves the exact values of A_i need not be determined but if all the conditions are to be satisfied and since the conditions are homogenous, the requirement that the coefficients be unique will lead to the following parameter relation:

$$M = \frac{4 D_1 \sinh \alpha \cosh \alpha + \frac{4}{3} D_2 \alpha \sinh \alpha}{\frac{1}{2} (\cosh \alpha - \frac{4}{3} \alpha \sinh \alpha) D_2 + \frac{1}{2} D_3 \sinh \alpha} \quad (26)$$

where D_1 , D_2 and D_3 are the following determinants:

$$D_1 = \det \begin{bmatrix} \cosh \alpha + \frac{1}{3} \alpha \sinh \alpha & \sinh \alpha & 2 \sinh \alpha \cosh \alpha \\ + B (\cosh \alpha - \frac{1}{3} \alpha \sinh \alpha) & & - \alpha \\ - \frac{1}{3} \alpha^2 \cosh \alpha & & \\ \frac{4}{3} \alpha (\sinh \alpha - \alpha \cosh \alpha) & 2 \alpha \cosh \alpha & 2 \cosh \alpha + 4 \alpha \sinh \alpha \\ K & -\frac{2PA}{\Delta f} \alpha - K \alpha & -\frac{2PA}{\Delta f} \sinh \alpha \\ & & - K \alpha \cosh \alpha \end{bmatrix} \quad (27)$$

$$D_2 = \det \begin{bmatrix} \alpha \cosh \alpha + B \sinh \alpha & \sinh \alpha & 2 \sinh \alpha \cosh \alpha - \alpha \\ 0 & 2\alpha \cosh \alpha & 2 \sinh \alpha \cosh \alpha + 4\alpha \sinh^2 \alpha \\ K\alpha & \frac{-2P\Lambda}{\Delta T} - K\alpha & \frac{-2P\Lambda}{\Delta T} \frac{\sinh \alpha}{\alpha} - K\alpha \cosh \alpha \end{bmatrix}$$

(28)

$$D_3 = \det \begin{bmatrix} \alpha \cosh \alpha + B \sinh \alpha & \cosh \alpha + B(\cosh \alpha - \frac{1}{3}\alpha \sinh \alpha) + \frac{1}{3}\alpha \sinh \alpha - \frac{1}{3}\alpha^2 \cosh \alpha & \sinh \alpha \\ 0 & \frac{4}{3}\alpha(\sinh \alpha - \alpha \cosh \alpha) & 2\alpha \cosh \alpha \\ K\alpha & K & \frac{-2P\Lambda}{\Delta T} \alpha - K\alpha \end{bmatrix}$$

(29)

This equation gives the required relationship between the Marangoni number and the wave number of the neutrally stable disturbances.

2.2 Constant Rate Solidification Process

A. The Mean State Solutions

The analysis performed in the previous section was for a stationary interface in which the solidification process entered only in the perturbation equations and not in the mean solution. Thus, the example does not realistically model a solidification process and was used only for the simplicity of the mathematics involved and for illustrative purposes. In this section the analysis of a more realistic

problem is presented. The problem will involve a continuous solidification process in which the melt is being fed continuously and at a constant rate while the solidification rate is proceeding also at a constant rate. A sketch of the problem is shown in Figure 3. However, in order to keep the solidification rate constant for a continuous process, it is required that the heat removal rate at the bottom of the solid be also constant. The physical analog of this model could be a continuous solidification process in which the melt is being replenished all the time in an exact amount to keep its mass constant for a very slow solidification process.

Thus, consider a finite depth melt which is infinite in the horizontal extent on top of a solid layer. The temperature distributions in both the solid and the liquid are given by the one-dimensional energy equations [Carslaw and Jaeger (1959)] in the form

$$\frac{\partial T_{ol}^*}{\partial t^*} - \left(\frac{\rho_s k_l}{\rho_l k_l} - 1 \right) \frac{dS}{dt^*} \frac{\partial T_{ol}^*}{\partial z^*} = \kappa_l \frac{\partial^2 T_{ol}^*}{\partial z^{*2}} \quad (30)$$

$$\frac{\partial T_{os}^*}{\partial t^*} = \kappa_s \frac{\partial^2 T_{os}^*}{\partial z^{*2}} \quad (31)$$

where ρ_s and ρ_l are the densities of the solid and liquid, respectively, and the rest of the notation is the same as that used in the previous section. Note that here the interface position $S(t)$ is a function of time and not a constant as before. However, it will be assumed from the start that the interface moves at a constant speed v_p , where

$$\frac{dS}{dt^*} = v_p \quad (32)$$

At this point, as will prove beneficial later, the origin of the coordinates is moved to the solid-liquid interface via the following Galilean transformation:

$$\begin{aligned} t^* &= t \\ z^* &= z - v_p t \end{aligned} \quad (33)$$

This transformation will render equations (30) and (31) to the following form:

$$-v_p \frac{\rho_s}{\rho_l} \frac{dT_{0l}^*}{dz^*} = \kappa_l \frac{d^2 T_{0l}^*}{dz^{*2}} \quad (34)$$

$$-v_p \frac{dT_{0s}^*}{dz^*} = \kappa_s \frac{d^2 T_{0s}^*}{dz^{*2}} \quad (35)$$

Also in these equations the primes have been dropped for ease of notation.

The boundary conditions appropriate to this problem are the following:

$$\left. \begin{aligned} T_{0s}^* &= T_{0l}^* = T_m^* \\ k_s \frac{dT_{0s}^*}{dz^*} - k_l \frac{dT_{0l}^*}{dz^*} &= -\rho_s L v_p \end{aligned} \right\} z^* = 0 \quad (36)$$

$$T_{0l}^* = T_2^* ; \quad z = d \quad (37)$$

$$q_{0s} = k_s \frac{dT_{0s}^*}{dz^*} ; \quad z^* = -v_p t \quad (38)$$

Note that for the solid boundary condition a heat transfer rate condition is used rather than a fixed temperature condition in order to be consistent with the assumption of a constant solidification rate.

The temperature distribution in the liquid phase may be obtained from the solution of the above system to be:

$$T_{ol} = [1 - \exp(-v_p \rho z / k_l)] [1 - \exp(-v_p \rho d / k_l)]^{-1} \quad (39)$$

where T_{ol} and z are dimensionless quantities having the following form:

$$z = z^* / d \quad ; \quad T_{ol} = \frac{T_{ol}^* - T_m^*}{T_z^* - T_m^*}$$

A plot of this distribution of temperature is given in Figure 4. The system of equations and the boundary conditions also specify uniquely the temperature distribution in the solid and the propagation speed of the interface. However, use will be made of the latter condition which is also a matching condition and will be written out when the need arises.

B. Linear Stability Analysis

As indicated earlier, the stability of the solid-liquid interface is inferred from the stability of the liquid phase. The stability analysis here is performed in a very similar manner as was done in the previous section. Again, the temperature and velocity fields are separated into a mean and a perturbation and substituted into the momentum and energy equations resulting in a linearized form for the equations for the perturbation functions. In this case, however,

a Galilean transformation is again adopted as was done for the mean temperature distribution where

$$\begin{aligned}t^* &= t^* \\x^* &= x^* \\z^* &= z^* - v_p t^*\end{aligned}$$

Also, the resulting independent variables in the new frame of reference are non-dimensionalized in the following way:

$$t = t^* v_p / d$$

$$[x, y, z] = [x^*/d, y^*/d, z^*/d]$$

$$\vec{u} = \vec{u}^* / v_p$$

where d is the depth of the liquid layer.

The resulting linear non-dimensional governing equations for the perturbation functions are

$$\left[\frac{\partial}{\partial t} - \frac{R_s}{S_1} \frac{\partial}{\partial z} - \left(\frac{v}{v_p d} \right) \nabla^2 \right] \nabla^2 w' = 0, \quad (40)$$

$$\left[\frac{\partial}{\partial t} - \frac{R_s}{S_1} \frac{\partial}{\partial z} - \left(\frac{v_c}{v_p d} \right) \nabla^2 \right] T_1' = -w' \frac{dT_{01}}{dz} \quad (41)$$

$$\left[\frac{\partial}{\partial t} - \frac{\partial}{\partial z} - \left(\frac{K_s}{v_p d} \right) \nabla^2 \right] T_s' = 0 \quad (42)$$

Most boundary conditions under which the above equations are to be solved in the moving frame of reference are identical to conditions (10)-(16) except for condition (16) which now is given by

$$k_s \frac{\partial T_s'}{\partial z} - k_l \frac{\partial T_l'}{\partial z} = -\rho_l L \omega'$$

Again, due to the form of the boundary conditions, equations (40)-(42) may be solved through the normal mode method. It will be assumed for simplicity that the perturbation functions are two-dimensional. Under these circumstances the perturbation functions will take the same form as (17). Substituting this functional form of the solution into equations (40)-(42) we get after setting $a_0 = 0$:

$$\left[\frac{1}{\rho} D + \frac{1}{R} (D^2 - \alpha^2) \right] (D^2 - \alpha^2) \psi = 0 \quad (43)$$

$$\left[\frac{1}{\rho} D + \frac{1}{\rho_r R} (D^2 - \alpha^2) \right] \theta_l = \frac{dT_{0l}}{dz} \psi \quad (44)$$

$$\left[D + \frac{\Delta}{\rho_r R} (D^2 - \alpha^2) \right] \theta_s = 0 \quad (45)$$

where

$$R = v_p d / \nu$$

In equations (43)-(45) we have again invoked the principle of exchange of stability.

The solution method for the system of equations (43)-(45) is slightly different here from that of the previous case. First,

equation (43) is solved alone for the velocity perturbation $v(z)$.

Then equation (44) is solved for the temperature perturbation $\theta_0(z)$

as an inhomogenous equation. Equation (45), however, is uncoupled

and may be solved separately. The solution for equation (43) may be

easily written in the form

$$v(z) = \sum_{i=1}^4 A_i \exp(\lambda_i z) \quad (46)$$

where λ_i are given by

$$\begin{aligned} \lambda_{1,2} &= \pm \alpha \\ \lambda_{3,4} &= -\frac{1}{2} \frac{R}{\rho} \pm \frac{1}{2} \left\{ \left(\frac{R}{\rho} \right)^2 + 4\alpha^2 \right\}^{1/2} \end{aligned} \quad (47)$$

while the solution to equation (44) is given by

$$\theta_0(z) = \sum_{i=1}^4 A_i C_i \exp[(\lambda_m + \lambda_i)z] + \sum_{i=5}^6 A_i \exp(\lambda_i z) \quad (48)$$

where A_1 through A_4 and λ_1 through λ_4 are the same constants as those

in the velocity distribution, while λ_5 and λ_6 are given by

$$\lambda_{5,6} = -\frac{Pr R}{2\rho} \pm \frac{1}{2} \left\{ \left(\frac{Pr R}{2\rho} \right)^2 + 4\alpha^2 \right\}^{1/2} \quad (49)$$

The C_i appearing in (48) are given by

$$C_i = A_m \left\{ (\lambda_m + \lambda_i) / \rho + \frac{1}{Pr R} \left[(\lambda_m + \lambda_i)^2 - \alpha^2 \right] \right\}^{-1} \quad (50)$$

$i = 1, \dots, 4$

where

$$A_m = \frac{P_r R}{\rho} \{1 - \exp(-R P_r / \rho)\}^{-1}$$

$$\lambda_m = R P_r / \rho$$

(51)

Since the solution for the perturbation velocity and temperature are obtained separately it is instructive to give the boundary conditions in terms of both variables. These are

$$\theta_1(0) = 0$$

$$\theta_2(0) = 0$$

$$\partial v(0) = 0$$

$$\partial \theta_1 - \frac{\mathcal{L}}{K} v(0) = 0$$

$$v(1) = 0 \quad ; \quad \theta_2(-\beta v_p) = 0$$

$$\partial \theta_1(1) + \beta \theta_2(1) = 0$$

$$(\mathcal{N}^2 + \alpha^2) v(1) - \mathcal{M} \alpha^2 \theta_1(1) = 0$$

(52)

where

$$\mathcal{L} = \Lambda P_r C K$$

$$\mathcal{M} = (\partial \sigma / \partial T) \frac{(T_2^* - T_m^*)}{\mu v_p}$$

$$C = c_{p1} / c_{ps}$$

Thus substituting the solutions given by (46) and (48) into the boundary conditions (52) yields a system of equations for A. If the value of the coefficients A_i is to be unique then the determinant of the coefficient matrix for A_i must be zero, i.e.,

$$\det [E] = 0$$

(54)

where the matrix E is given by

$$\begin{bmatrix}
 C_1 & C_2 & C_3 & C_4 & 1 & 1 \\
 \lambda_1 & \lambda_2 & \lambda_3 & \lambda_4 & 0 & 0 \\
 \exp(\lambda_1) & \exp(\lambda_2) & \exp(\lambda_3) & \exp(\lambda_4) & 0 & 0 \\
 (\lambda_m + \lambda_1)C_1 & (\lambda_m + \lambda_2)C_2 & (\lambda_m + \lambda_3)C_3 & (\lambda_m + \lambda_4)C_4 & \lambda_5 & \lambda_6 \\
 (\lambda_m + \lambda_1 + \beta)C_1 x & (\lambda_m + \lambda_2 + \beta)C_2 x & (\lambda_m + \lambda_3 + \beta)C_3 x & (\lambda_m + \lambda_4 + \beta)C_4 x & (\lambda_5 + \beta) & (\lambda_6 + \beta) \\
 \exp(\lambda_m + \lambda_1) & \exp(\lambda_m + \lambda_2) & \exp(\lambda_m + \lambda_3) & \exp(\lambda_m + \lambda_4) & & \\
 z\alpha^2 \exp(\lambda_1) & z\alpha^2 \exp(\lambda_2) - \mathcal{M}x & (\lambda_3^c + \alpha^c) \exp(\lambda_3) & (\lambda_4^c + \alpha^c) \exp(\lambda_4) & -\mathcal{M}\alpha^c \exp(\lambda_5) & -\mathcal{M}\alpha^c x \\
 -\mathcal{M}\alpha^c C_1 \exp(\lambda_m + \lambda_1) & \alpha^c C_2 \exp(\lambda_m + \lambda_1) & -\mathcal{M}\alpha^c C_3 \exp(\lambda_3 + \lambda_m) & -\mathcal{M}\alpha^c C_4 \exp(\lambda_m + \lambda_4) & & \exp(\lambda_6)
 \end{bmatrix}$$

To obtain the neutral stability curves equation (54) is then solved for one of the parameters in terms of the rest, i.e.,

$$M = f(P_r, R, P, \Lambda, B, K, C, \alpha, Q). \quad (56)$$

3. Non-Dimensional Parameters

The goal of the present work is to calculate the neutral stability curves and the critical Marangoni number, M , as a function of the non-dimensional wave number of the disturbance. It was necessary to non-dimensionalize the problems to be able to make these calculations. There are always many ways to non-dimensionalize a problem, but the method used recover familiar dimensionless parameters plus additional parameters.

3.1. Steady State Process

The dimensionless independent variables were defined along with the solution to the problem given earlier. The dependent variables were non-dimensionalized to give the following relationship for the neutral stability curve:

$$M = M(\alpha, B, \Lambda, \gamma, \Delta, K)$$

where

$$M = \frac{d\sigma}{dT^*} \frac{dT_{o\ell}^*}{dz^*} d^2}{\mu_\ell \kappa_\ell}$$

$$\alpha = dk = \frac{2\pi d}{\lambda} = \text{dimensionless wave number } (\lambda = \text{disturbance wave length, } k = \text{disturbance wave number})$$

$$B = \frac{gd}{k_\ell} = \text{Biot modulus}$$

$$\Lambda = \frac{L}{C_{ps} (T_2^* - T_1^*)}$$

$$\gamma = \frac{dT_{o\ell}^*}{dz}$$

$$\Delta = \kappa_s / \kappa_l$$

$$K = k_l / k_s$$

It was desirable to calculate the neutral stability curves using values of these parameters which characterize material systems of interest for space processing. Table I lists property values for some metallic materials that would be of interest. The parameters Δ and K depend only upon the material properties and their values are tabulated in Table II. Δ varies from 0.7 to 3.0 for the metals considered, while K varies from 0.44 to 1.74 but is generally around 0.5.

The remaining dimensionless parameters depend upon the boundary conditions of the problem as well as the material properties. First consider the mean temperature field. The analysis assumed that the material properties were constant but in fact they are strong functions of temperature. Therefore, for this reason and because solidification usually proceeds slowly, the temperature difference across the liquid-solid system can be assumed to be small, say, 2°C. Then Λ varies from 35 to 200 and γ from 1.2 to 1.5.* The Biot modulus, B , on the other hand, which characterizes the heat transfer through the upper liquid surface, can be left as a parameter in the problem.

Smaller values of Λ correspond to large values of $(T_2^ - T_1^*)$ and cannot be expected to yield satisfactory results using the present analysis.

3.2. Constant Rate Process

For the continuous rate process the neutral stability curve is given by the following relation:

$$M = M(\alpha, R, Pr, Q, B, \Lambda, K, P, C)$$

where

$$R = \frac{v_p d}{\nu_l} = \text{Reynolds number}$$

$$Pr = \frac{\nu_l}{\kappa_l} = \text{Prandtl number}$$

$$P = \rho_l / \rho_s$$

$$C = C_{p_l} / C_{p_s}$$

$$Q = \frac{q_{os} d}{k_l (T_2^* - T_m^*)}$$

$$\Lambda = \frac{L}{C_{p_s} (T_2^* - T_m^*)}$$

and K and B are defined as before. Notice that Λ is now defined in terms of $T_2^* - T_m^*$ and is thus different from the parameter defined for the steady state problem. M is defined as

$$M = \frac{(T_2^* - T_m^*) \frac{d\sigma}{dT^*}}{\mu_l v_p}$$

If a mean temperature gradient in the liquid defined by

$$\overline{\frac{dT^*}{dz^*}} = \frac{(T_2^* - T_m^*)}{d}$$

is used in the definition of the Marangoni number, then M is related to it as follows:

$$M = R Pr M$$

However, M is the more natural parameter for the analysis and the neutral stability curves will be given in terms of it. Since Pr is small M is considerably smaller than M , for Reynolds numbers of the order of one.

The continuous rate problem was non-dimensionalized using the speed of the phase plane, v_p , as one of the parameters in (M and R). The phase plane speed is not one of the boundary conditions of the problem but rather is part of the solution. It is determined from the non-linear matching condition that results from matching the solutions at the liquid-solid interface for the mean motion. That matching condition is the following:

$$q_{os} \exp\left(-\frac{v_p d}{\chi_s}\right) + \frac{k_l \rho_l v_p (T_2^* - T_m^*)}{\rho_s \chi_l \left[1 - \exp\left(-\frac{v_p \rho_l d}{\rho_s \chi_l}\right)\right]} = \rho_s L v_p.$$

This relation can be non-dimensionalized using the parameters listed above and they were selected, in part, to accomplish that non-dimensionalization. In non-dimensional form the equation becomes

$$\frac{QPC}{\Delta R Pr} \exp\left(-\frac{R Pr}{\Delta}\right) + \frac{P^2 C}{\Delta [1 - \exp(-R Pr)]} = 1.$$

From Table II it can be seen that $Pr = p(10^{-2})$, $\Delta = 0(1)$, and $P = 0(1)$. Therefore, the exponentials are small if $R = 0(1)$. $R = v_p d / v_l$. From Table I, $v_l = 0(10^{-2})$ and for a typical

system $d = 0(1 \text{ cm})$ and v_p will be of the order of 10^{-2} cm/sec if R is of the order of one.

Therefore, for $R = 0(1)$ the above expression can be linearized, yielding the following expression for the Reynolds number in terms of material properties and the boundary conditions of the problem.

$$R = \frac{PC}{Pr} \left(\frac{Q+1}{QK+\Lambda} \right).$$

Values of the parameters for some metallic materials are given in Table II. The above expression is used to calculate R in terms of the other given parameters. Pr , P and C depend only upon the properties of the materials. Q , which is the non-dimensional heating rate, fixes the rate of solidification and can be independently varied. B , which determines the perturbation heat transfer rate, can also be kept as a parameter in the solution.

4. Discussion

It is a common practice in stability analyses to present the results in the form of neutral stability curves such as shown in Figure 5. Such curves delineate in the relevant parameter space regions of stability and instability. It should be emphasized that the information obtained from such curves is the most that one can hope to get from linear stability analyses. However, it should be remembered that in obtaining such information the principle of exchange of stability has been used without any proof on its validity for the present problem, although it is felt that it may hold here. For more information on the ensuing process, whether in the form of a stationary time periodic bifurcated solution or a totally unstable solution, resort must be made to nonlinear analysis. Thus, the information obtained here is just qualitative in nature without any detail on the ensuing flow, if it occurs.

4.1 Steady State Process

The neutral stability curves for the steady state solidification process given by equation (26) are shown in Figure 5. All of these curves show a critical Marangoni number indicating a range of Marangoni numbers, M , for which the perturbations are stable regardless of the wave number. The various curves are of different values of the Biot modulus, B , which is a non-dimensional form of the rate of heat transfer through the upper liquid surface. The similarity between this figure and Figure 1 of Pearson (1958) is striking. However, this similarity is

expected since the problem solved here is almost identical with that of Pearson. The only difference between the two is in the form of the energy balance condition (16), whereby Pearson's condition is recovered when the latent heat parameter $\Lambda \rightarrow \infty$. In fact, this is exactly what happens, for as Λ becomes large, Pearson's stability curves for the ideally conducting case are recovered. However, this result is achieved quite fast and there exists differences only for unrealistically small values of Λ , i.e., Λ values of order 1. For any realistic solidification process in which the temperature gradient in the liquid phase is not too high, the value of Λ is of order 10 to 100. The conclusion to be drawn here is that the system becomes more unstable (shifting of the neutral stability curves to the left) with a decrease in the latent heat values.

4.2 Constant Rate Process

The neutral stability curve is given as the function

$$M = M(\alpha)$$

with Pr , Q , B , Λ , K , P , and C as parameters. Pr , K , P , and C depend only upon the properties of the materials and neutral stability curves were computed for typical values of these quantities (see Table II). The dependence of the neutral stability curve on each of these parameters was examined and will be described below. Although the problem examined is greatly simplified compared to a realistic time-dependent solidification process, it is hoped that the dependence of the stability upon these parameters will be correctly predicted. All results are tabulated in Appendix III.

Increasing Q by increasing q_{0s} , which increases the rate of solidification, leads to lower critical values of M . Typical neutral stability curves are shown in Figure 7. The values of Q used correspond to very small values of q_{0s} , of the order of 0.1 to 0.5 joules/sec cm^2 . It is of interest to note that the wave number corresponding to M_{crit} is approximately constant (except as noted later) and equal to 2.0 to 2.2. This corresponds to a most critical wave length of about πd . This can be expected to be the dimension of the cellular pattern that would occur when M_{crit} is exceeded (Pearson (1958)).

Increasing the rate of heat transfer through the upper liquid surface, i.e., increasing B , stabilizes the flow (Figure 8). This conclusion is identical to that found in the steady state problem and by Pearson (1958) for a non-solidifying liquid. Furthermore, this latter result has been borne out by experiment. Notice now, however, that the wave number for the most critical disturbance increases with heating rate (Figure 9) and the convection cell size can be expected to decrease accordingly. B can be varied by changing either the depth of the liquid or the heat transfer coefficient, q , and its variation has no effect on the solidification rate R .

Λ can be changed in two ways and they have different influences upon the stability of the system. Different materials will have different values of L/C_{ps} (Table II) and this will result in different values of Λ , for a given $(T_2^* - T_m^*)$. Keeping all other boundary conditions constant still results in a change in R . The effect of the change in L/C_p upon M_{crit} is shown in

Tabel IV and Figure 10. Materials with higher values of L/C_{ps} are more stable, even though the rate of solidification is also in general faster.

Λ can also be varied by changing $(T_2^* - T_m^*)$ but that also changes Q . The effect of changing $(T_2^* - T_m^*)$ in Λ and Q simultaneously, while keeping the other boundary conditions constant, is shown in Table IV and Figure 11. Again, increasing Λ , through decreasing $(T_2^* - T_m^*)$, stabilizes the flow.

As noted above, the parameters Pr , K , P , and C are constant for a given material. However, the sensitivity of the stability upon these parameters was examined so that comparison could be made of the relative stability of different materials.

The Prandtl number can vary over many orders of magnitude, depending upon the material (Table II). Because the Reynolds number is directly proportional to Pr , calculations were performed at constant $R = 1.0$ by varying Λ simultaneously with Pr . The variation of the critical value of M with Pr for this case is shown in Figures 12 and 13. Because the Maragoni number is related to M by

$$M = R Pr M$$

the variation in critical Marangoni number is very small. The results are summarized in Table V. These results are not accurate at the larger Pr because very large $(T_2^* - T_m^*)$ would be required to make Λ small enough to keep $R = 1.0$.

The effect of density and specific heat ratio, P and C , upon the critical value of M is shown in Figures 14 and 15. The greater the increase in the density of the material upon

solidification, i.e., the lower the value of P , the more stable the flow. Materials such as bismuth and water with values of P greater than one are somewhat less stable than materials with P less than one. Note that R increases somewhat as P is increased verifying the previous conclusion. The same conclusion can be drawn for increasing specific heat ratio, C (Figure 15). C also influences R but its effect is greater than the effect of changing R alone by changing Q .

K , the ratio of the coefficients of thermal conductivity, can be shown to have no effect upon the stability of the system.

5.0 Conclusions

The following conclusions can be drawn from the solution of these problems:

1. Increasing the heat transfer rate from the upper surface of the liquid by increasing the Biot modulus, B , stabilizes the flow. The wave number corresponding to the most unstable disturbance increases with B causing a corresponding decrease in convection cell size.

2. Increasing the rate of solidification by increasing the heat transfer rate through the solid (i.e., increasing Q by increasing q_{os}) destabilizes the flow. As Q increases the Reynolds number, R , is increased.

3. The wave number of the most unstable disturbance is about 2.0 to 2.2 for $B = 1.0$ and varies appreciably only with changes in B .

4. For a given temperature difference across the liquid, $(T_2^* - T_m^*)$, materials with larger values of L/C_{ps} are more stable than those with smaller values.

5. Decreasing $(T_2^* - T_m^*)$ while keeping other boundary conditions constant stabilizes the flow.

6. The Prandtl number, Pr , has little effect upon the critical Marangoni number for constant R .

7. Materials with larger values of density and specific heat ratios, P and C , are less stable than those with lower ratios.

8. The thermal conductivity ratio, K , has no effect on the stability of the flow.

References

- Boley, B.A. The Analysis of Problems of Heat Conduction and Melting, High Temperature Structures and Materials (Freudenthal, Boley & Liebowitz, ed.), Macmillan Co., New York, 260-315 (1964).
- Busse, F.H. and Schubert, G. Convection in a Fluid with Two Phases, J. Fluid Mech., 46, 801-812 (1971).
- Chang, C.E. and Wilcox, W.R. Analysis of Surface Tension Driven Flow in Floating Zone Melting, Int. J. Heat Mass Transfer, 19, 355-366 (1976).
- Carslaw, H.S. and Jaeger, J.C. Conduction of Heat in Solids, Oxford: Clarendon Press, Chapter XI (1959).
- Foust, O.J. Sodium NaK Engineering Handbook, Vol. 1, Sodium Chemistry and Physical Properties, Gordon and Breach (1972).
- Levich, V.G. and Krylov, V.S. Surface Tension-Driven Phenomena, Ann. Rev. Fluid Mech., 1, 293-316 (1969).
- Muehlbauer, J.C. and Sunderland, J.E. Heat Conduction with Freezing or Melting, App. Mech. Rev., 18, 951-959 (1965).
- Mullins, W.W. and Sekerka, R.F. Stability of a Planar Interface during Solidification of a Dilute Binary Alloy, J. App. Physics, 35, 444-451 (1964).
- Ockendon, J.R. and Hodgkins, W.R. Moving Boundary Problems in Heat Flow and Diffusion, Oxford U. Press (1975).
- Pearson, J.R.A. On Convection Cells Induced by Surface Tension, J.F.M., 4, 489-550 (1958).
- Rubinstein, L.I. The Stefan Problem, Trans. Math. Monographs, Vol. 27, Am. Math. Society (1971).
- Schubert, G.; Yuen, D.A.; Turcotte, D.L. Role of Phase Transition in a Dynamic Mantle, Geophys. J. R. Astr. Soc., 42, 705-735 (1975).
- Seki, N.; Fukusako, S.; Sugawara, M. A Criterion of Onset of Free Convection in a Horizontal Melted Water Layer with Free Surface, J. Heat Trans., 99, 92-98 (1977).
- Sparrow, E.M.; Schmidt, R.R.; and Ramsey, J.W. Experiments on the Role of Natural Convection in the Melting of Solids, J. Heat Trans., 100, 11-16 (1978).

Sparrow, E.M.; Patankar, S.V.; Ramadhyoni, S. Analysis of Melting in the Presence of Natural Convection in the Melt Region, J. Heat Trans., 99, 520-526 (1977).

Stefan, J. Uebereinige Probleme der Theorie der Wumeleitung, S.-B. Wien, Akad, Mat. Matus, 98, 173-484 (1889).

Turcotte, D.L. Geophysical Problems with Moving Phase Change Boundaries and Heat Flow, Moving Boundary Problems in Heat Flow and Diffusion (Ockendon & Hodgkins, ed.), Clarendon Press, Oxford, 91-102 (1975).

Ukanawa, A.O. Diffusion in Liquid Metal Systems, NASA Contractor Report, Contract NAS8-30252 (1975).

West, R.C. et al. Handbook of Chemistry and Physics, 54th Edition, CRC Press (1973).

Williams, F.A. Combustion Theory, Chap. 1, Addison-Wesley (1965).

Wolkind, D.J. and Segel, L.A. A Nonlinear Stability Analysis of the Freezing of a Dilute Binary Alloy, Phil. Trans. Roy. Soc. London, 268A, 351 (1970).

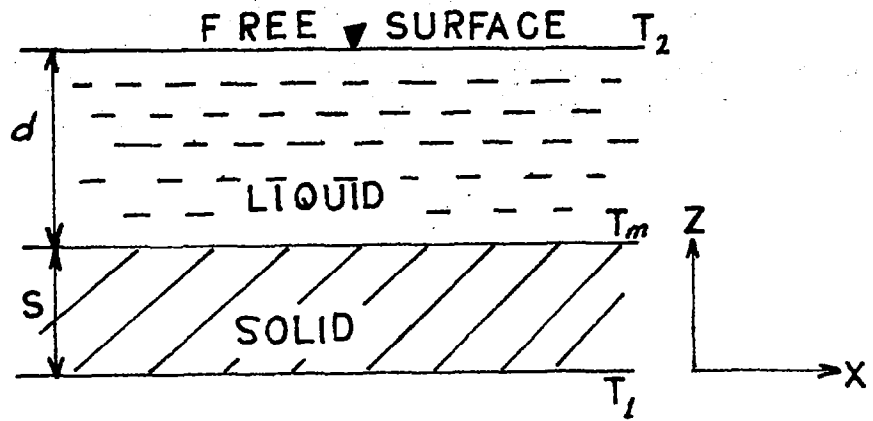


Figure 1. Problem Sketch for the Steady State Solidification Process

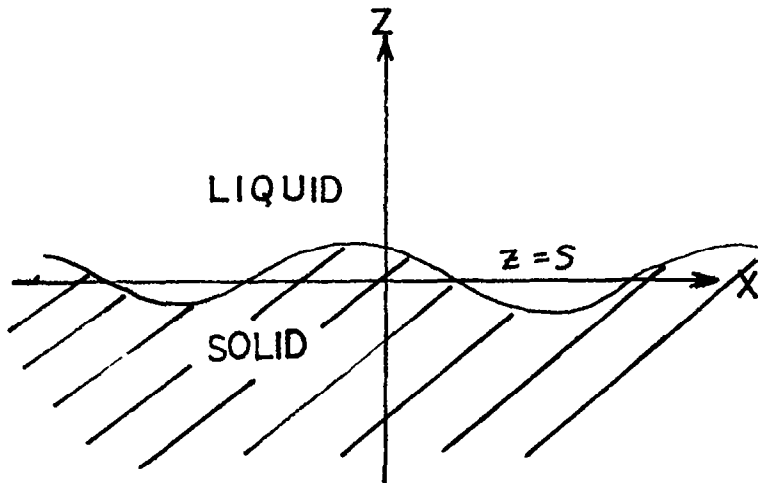


Figure 2. Sketch of the Deformation of the Liquid-Solid Interface Due to Convection in the Fluid

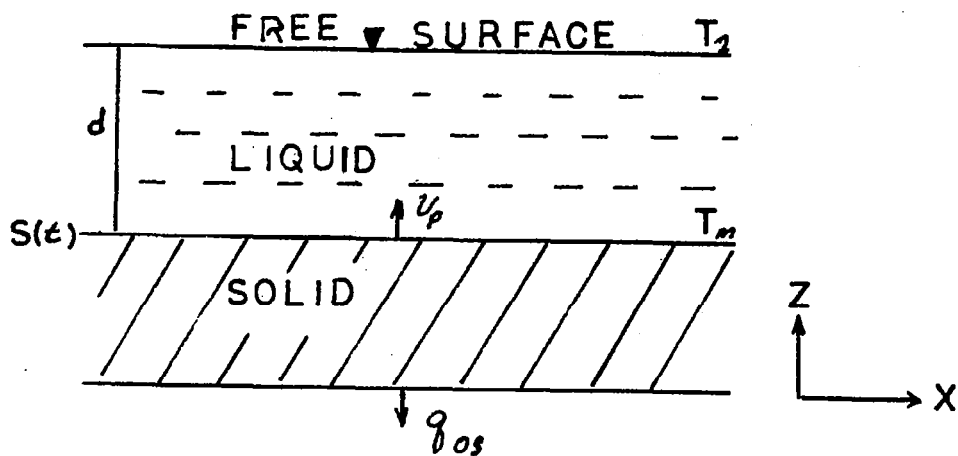


Figure 3. Problem Sketch for the Constant Rate Solidification Process

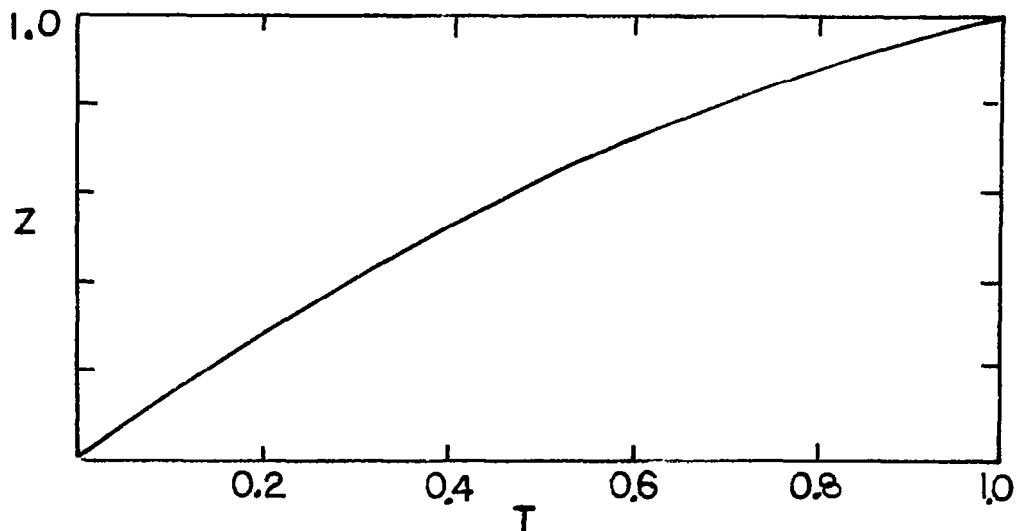


Figure 4. The Non-Dimensional Temperature Profile in the Liquid for the Constant Rate Solidification Process

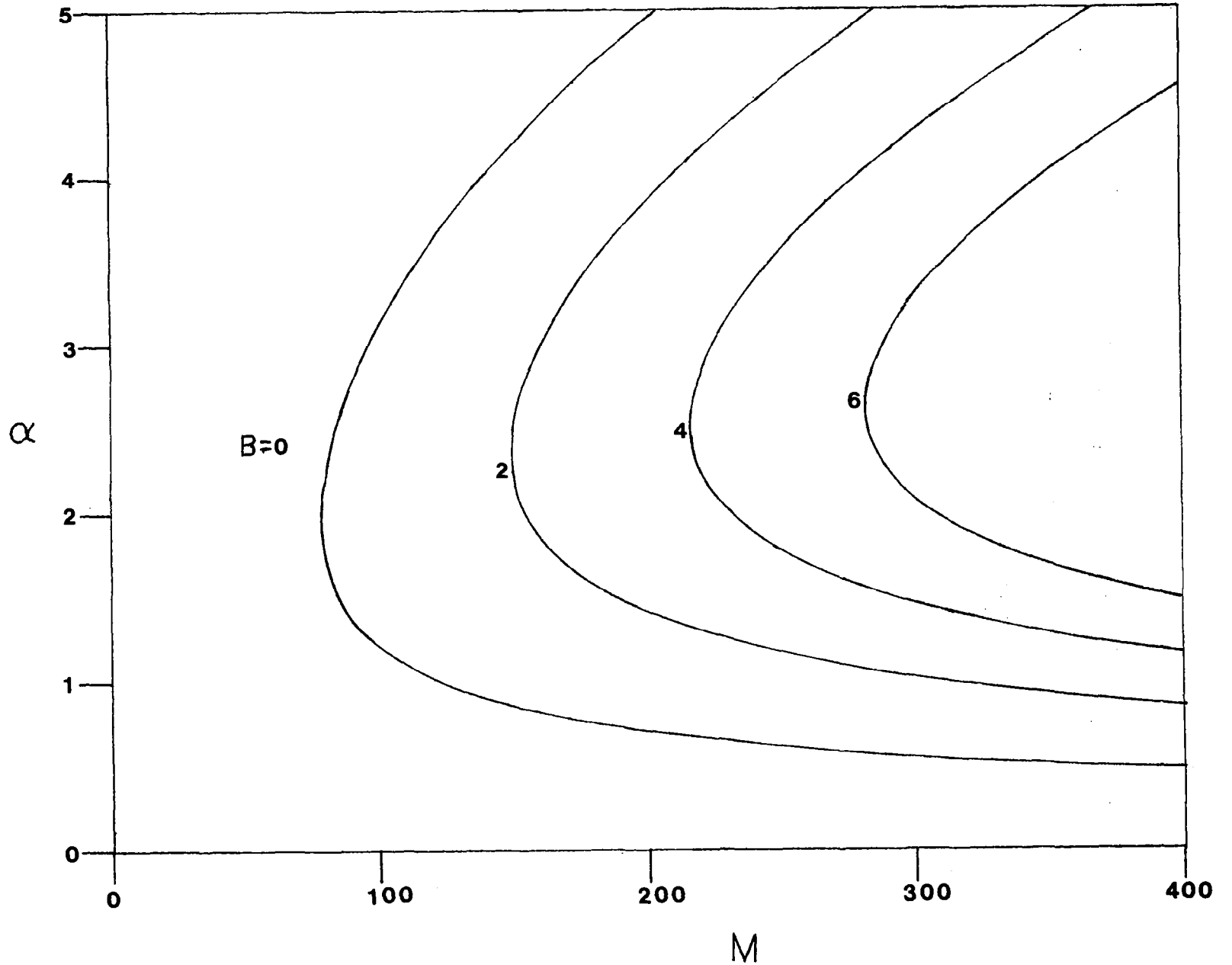


Figure 5. Effect of Biot modulus on the stability of the steady state process. $\Lambda = 20$, $\gamma = 1.2$, $K = 0.7$, $\Delta = 1.5$.

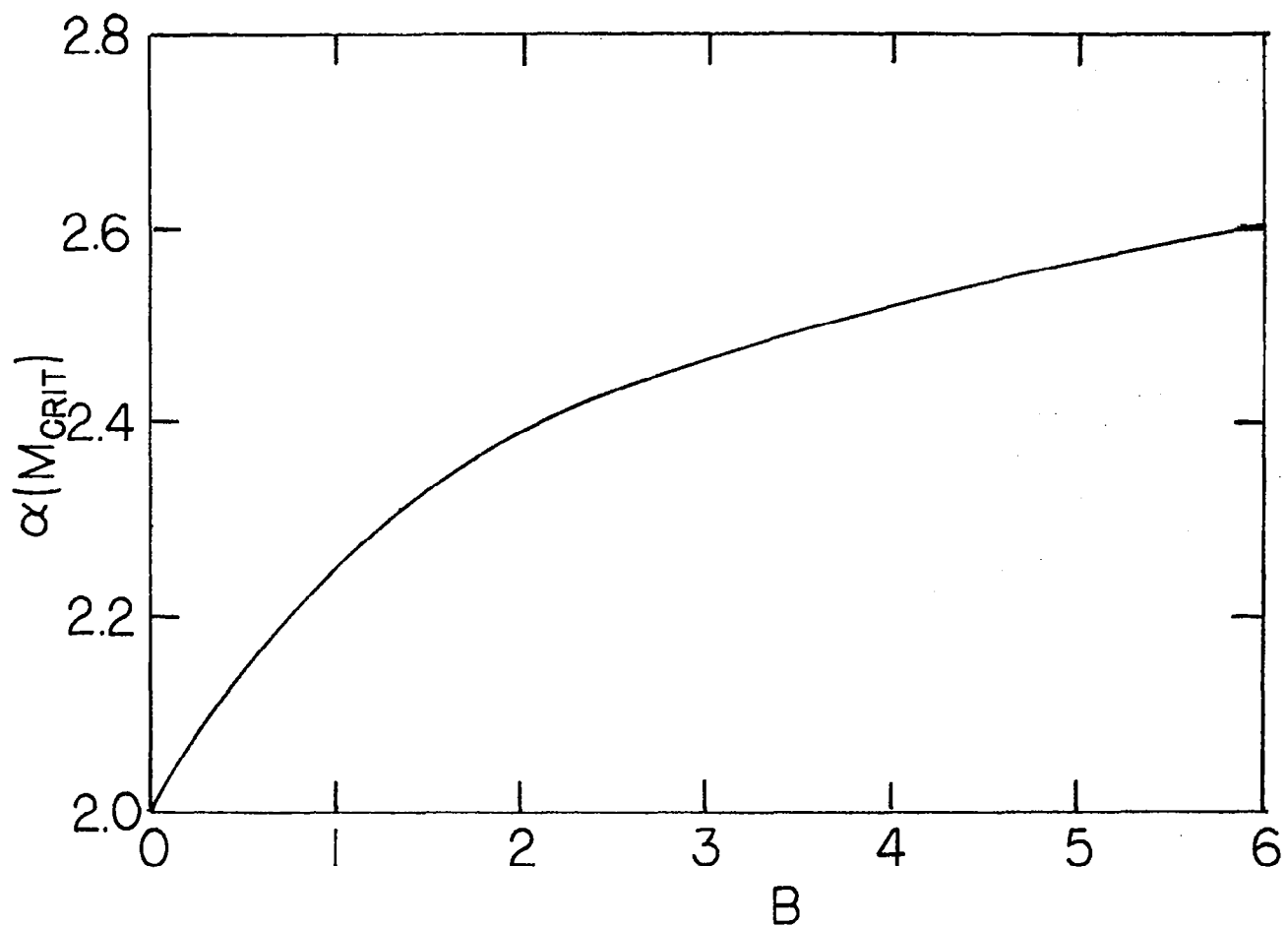


Figure 6. Variation of most unstable wave number with upper surface heat transfer rate for the steady state process. $\Lambda = 20$, $\gamma = 1.2$, $\Delta = 1.5$, $K = 0.7$.

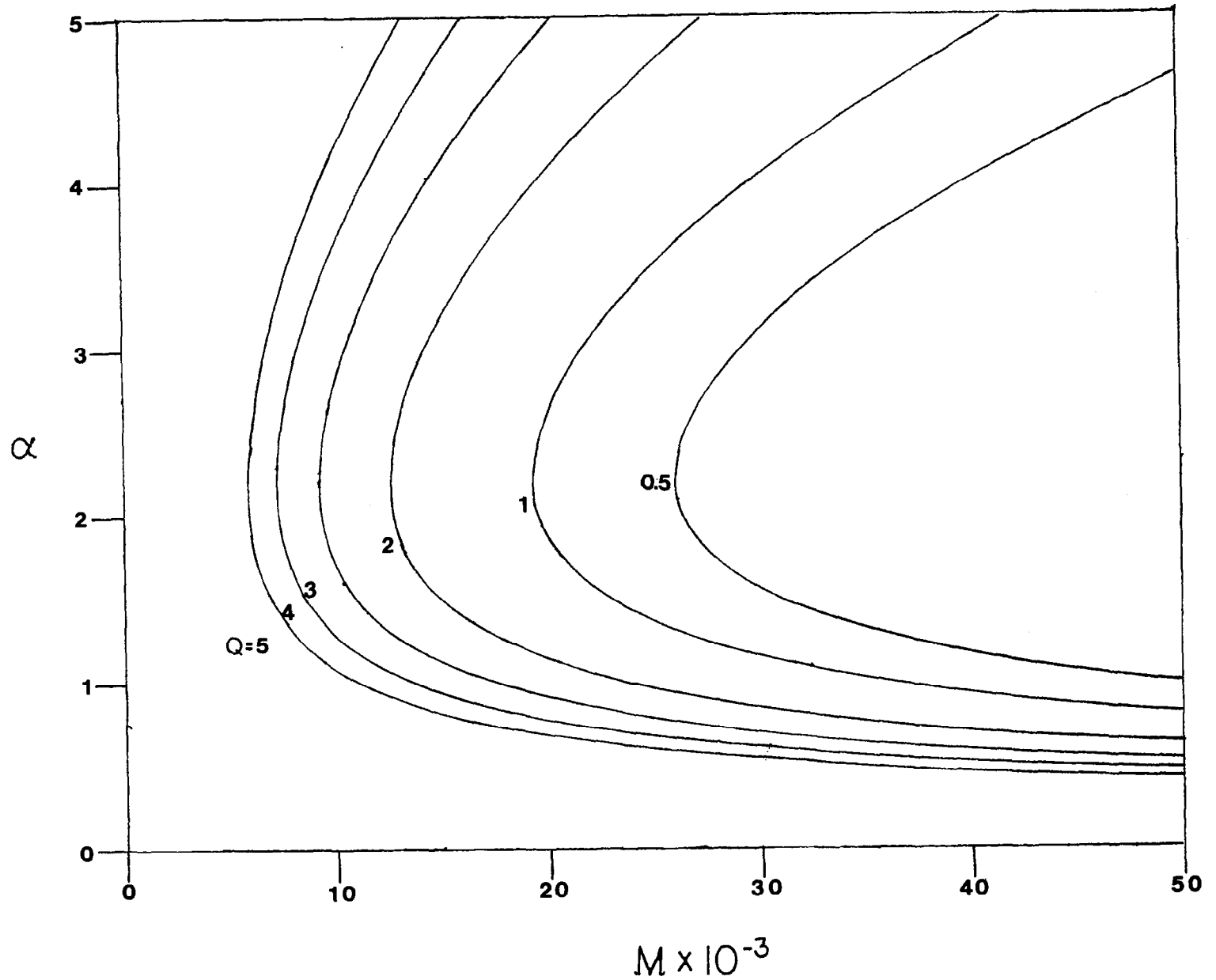


Figure 7. Effect of increasing the rate of solidification on the stability of the constant rate process. $P_r = 0.02$, $K = 0.5$, $P = 0.965$, $C = 1.04$, $\Lambda = 350$, $B = 1.0$.

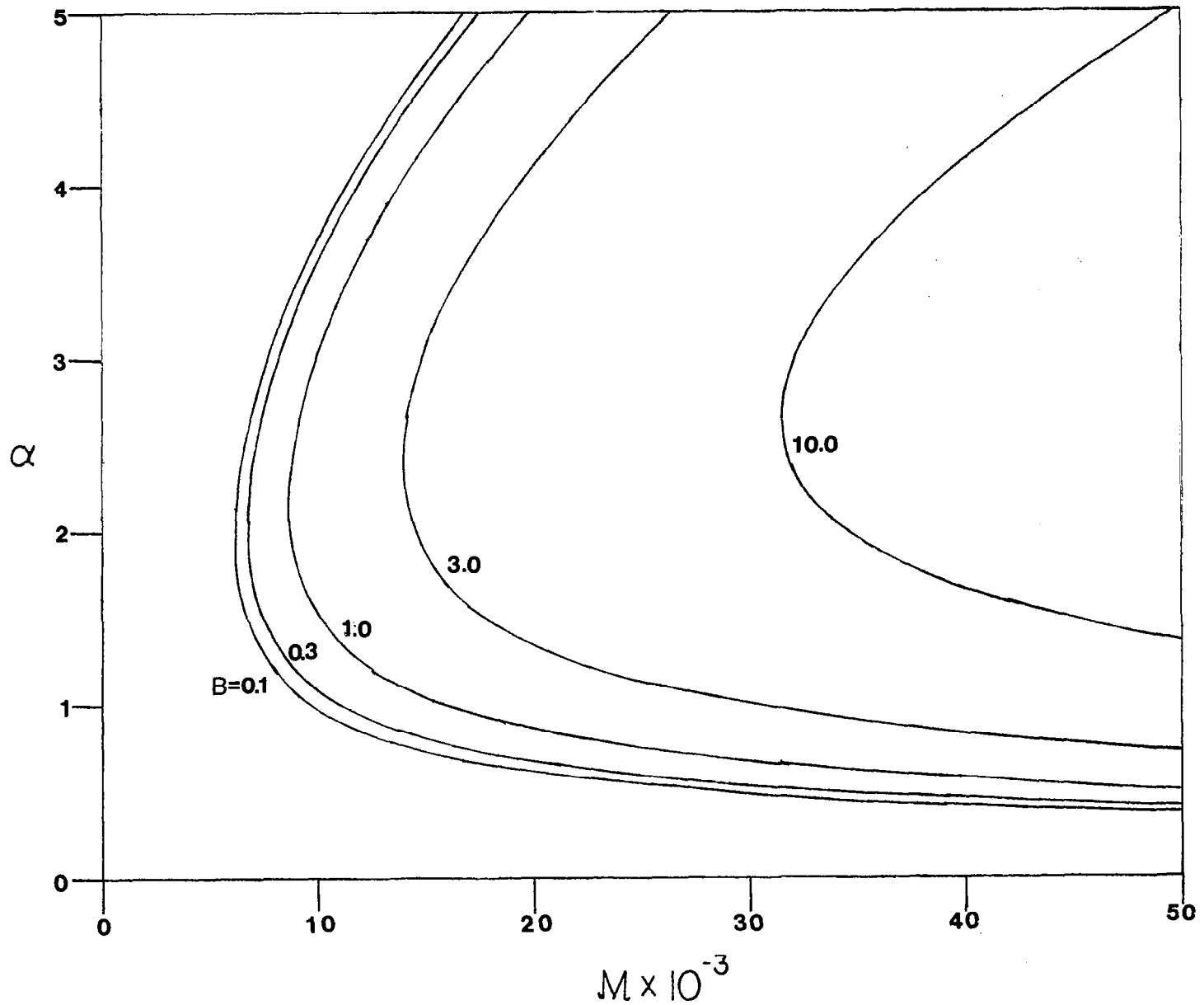


Figure 8. Effect of increasing the upper heat transfer rate on the stability of the constant rate process. $P_r = 0.01$, $K = 0.5$, $P = 0.975$, $C = 1.01$, $\Lambda = 175$, $Q = 1.0$.

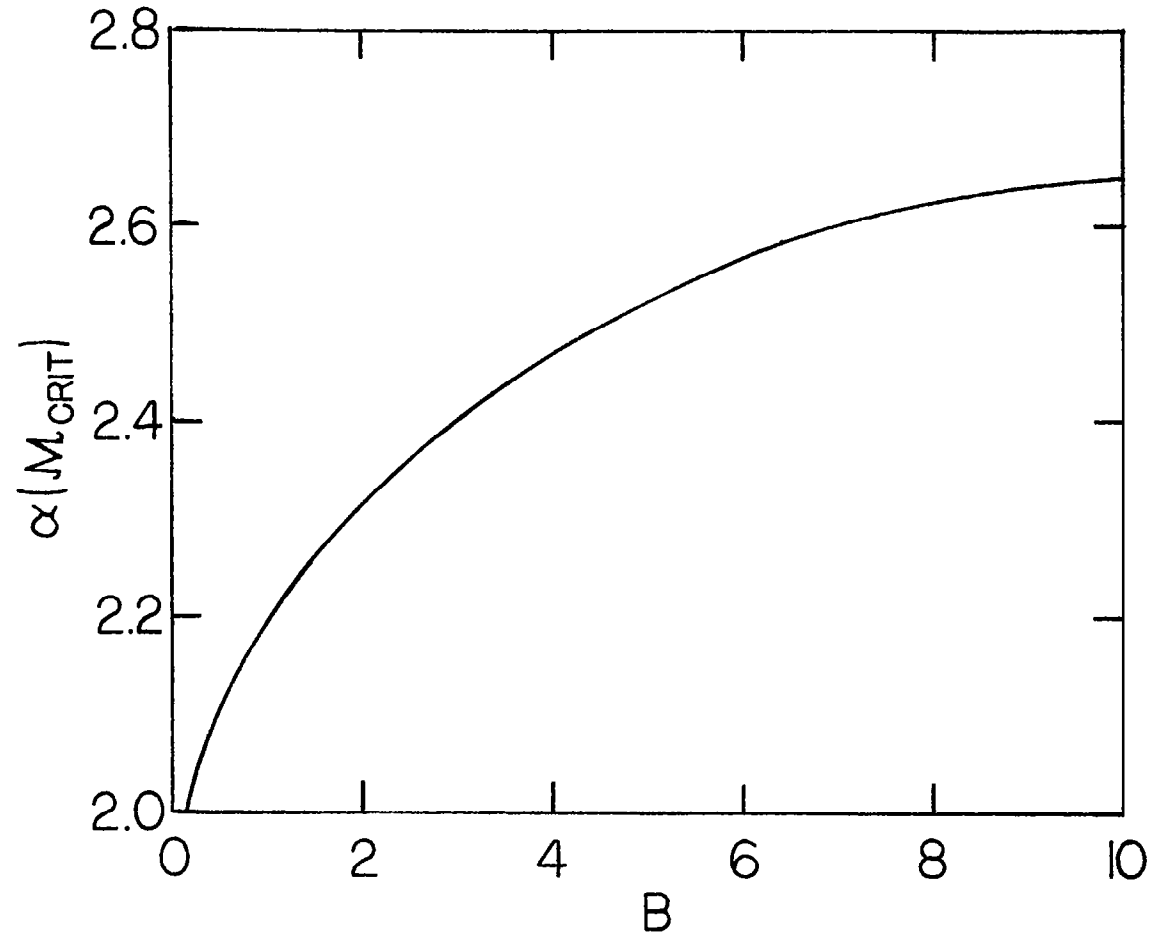


Figure 9. Variation of most unstable wave number with upper surface heat transfer rate for the constant rate process. $P_r = 0.01$, $\Lambda = 175$, $Q = 1.0$, $K = 0.7$, $P = 1.0$, $C = 1.0$, $R = 1.14$.

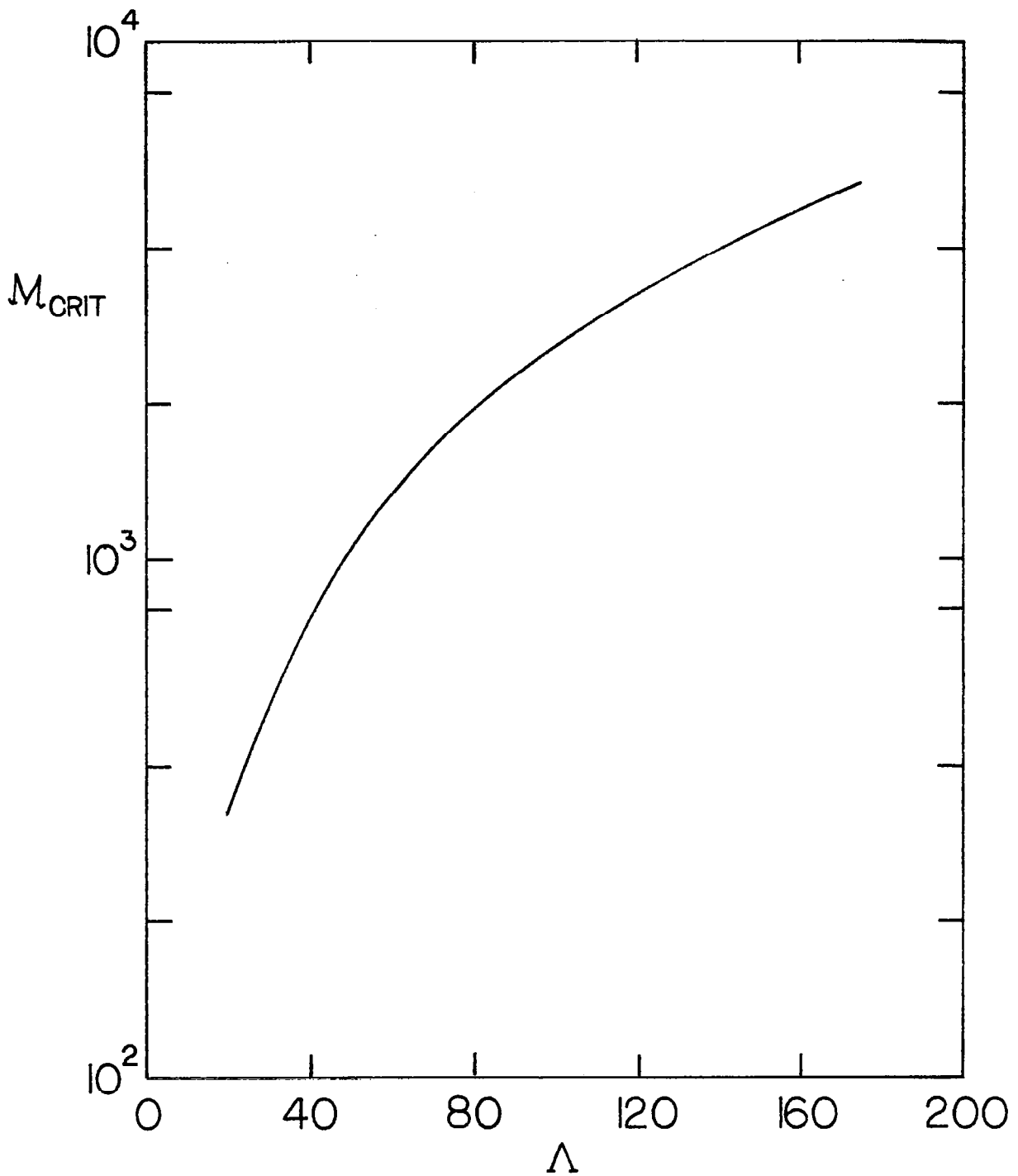


Figure 10. Effect of change in Λ (with constant $(T_2^* - T_m^*)$) upon M_{crit} for the constant rate process. $P_r = 0.01$, $Q = 2.0$, $K = 0.7$, $P = 1.0$, $C = 1.0$, $B = 1.0$.

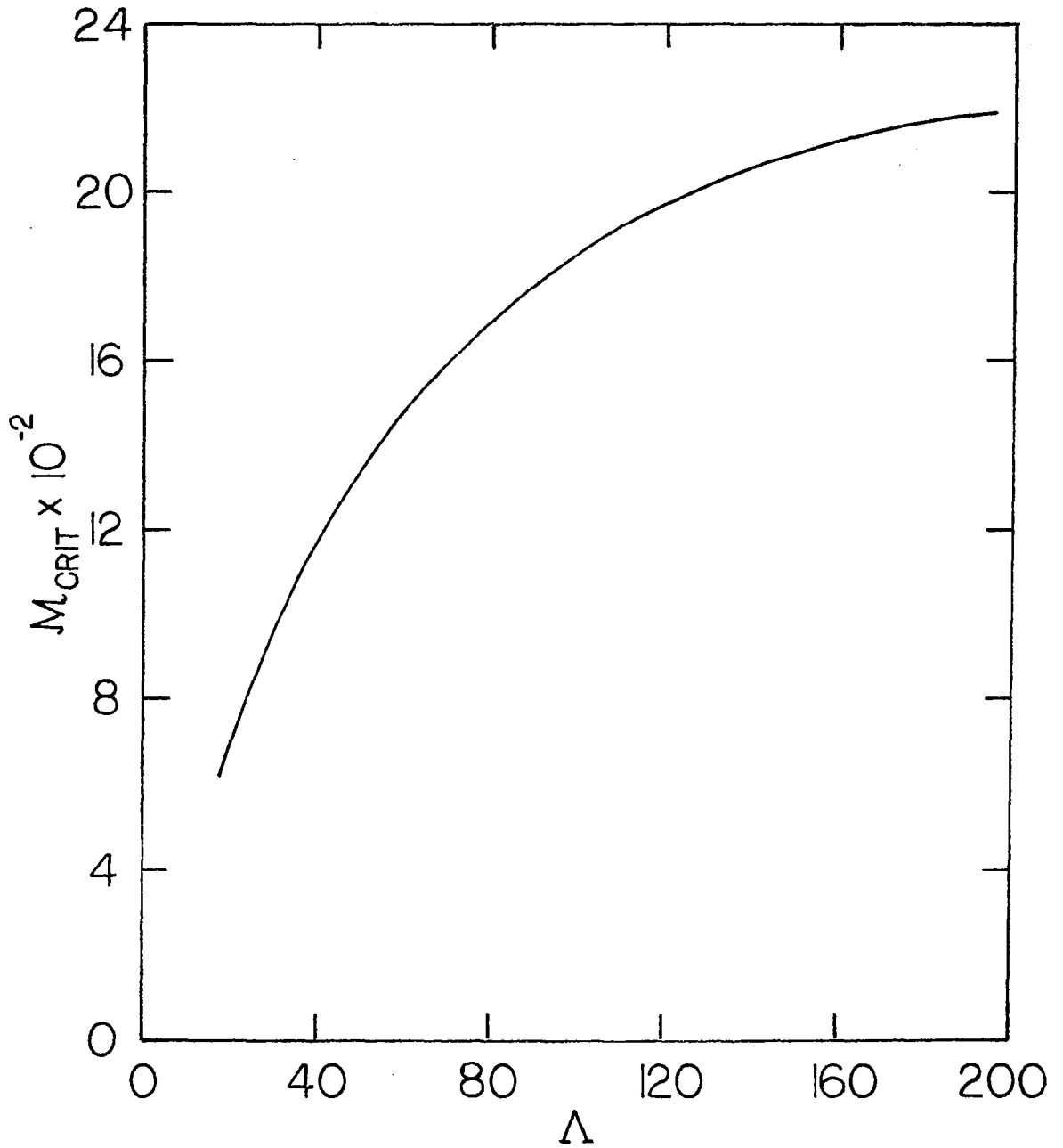


Figure 11. Effect of change in $(T_2^* - T_m^*)$ (with q_{0s} constant) upon M_{crit} for the constant rate problem. $Pr = 0.01$, $K = 0.7$, $P = 1.0$, $C = 1.0$, $B = 1.0$.

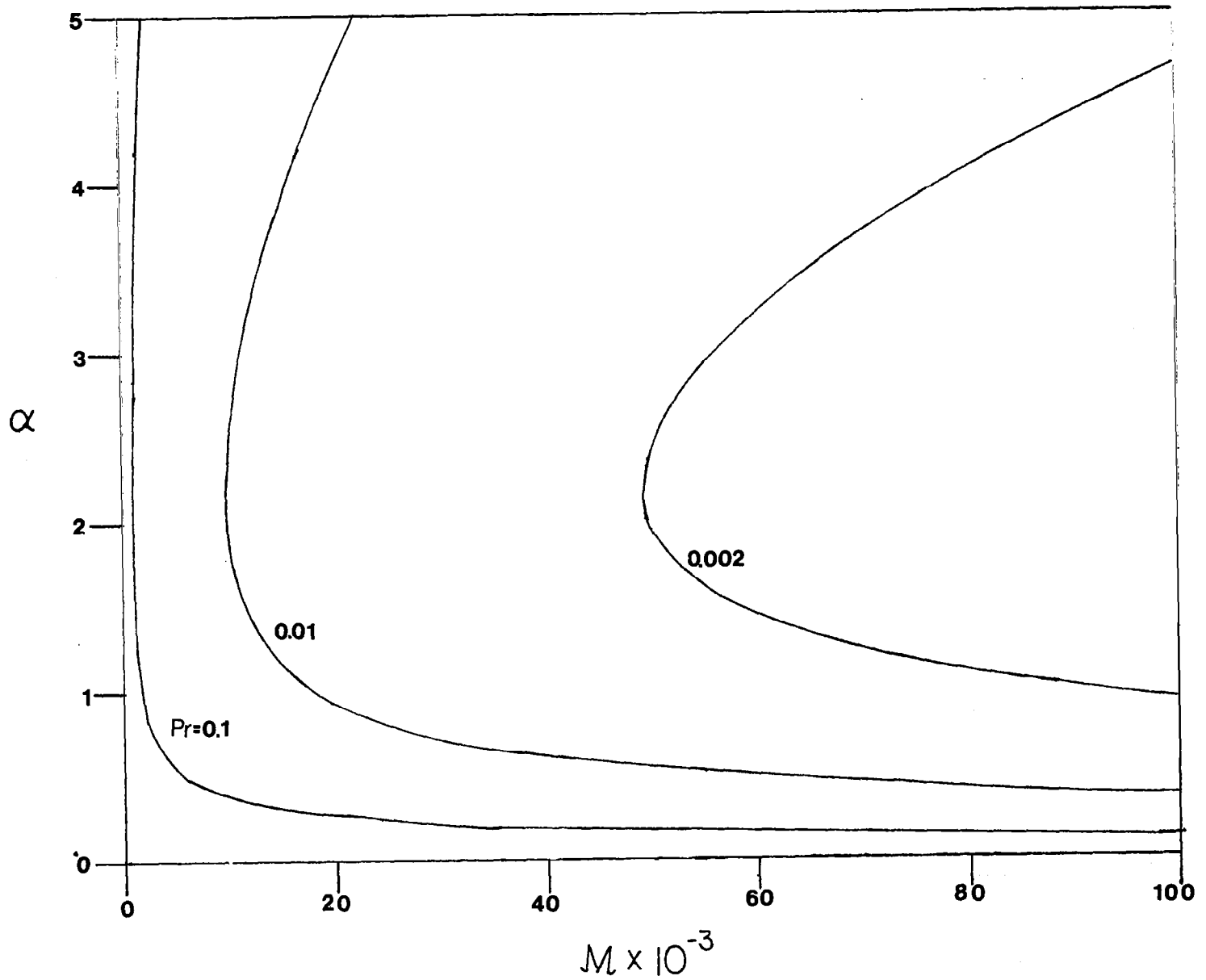


Figure 12. Comparison of the stability of materials of different Prandtl numbers for the constant rate process. $K = 0.7$, $P = 1.0$, $C = 1.0$, $Q = 1.0$, $R = 1.0$.

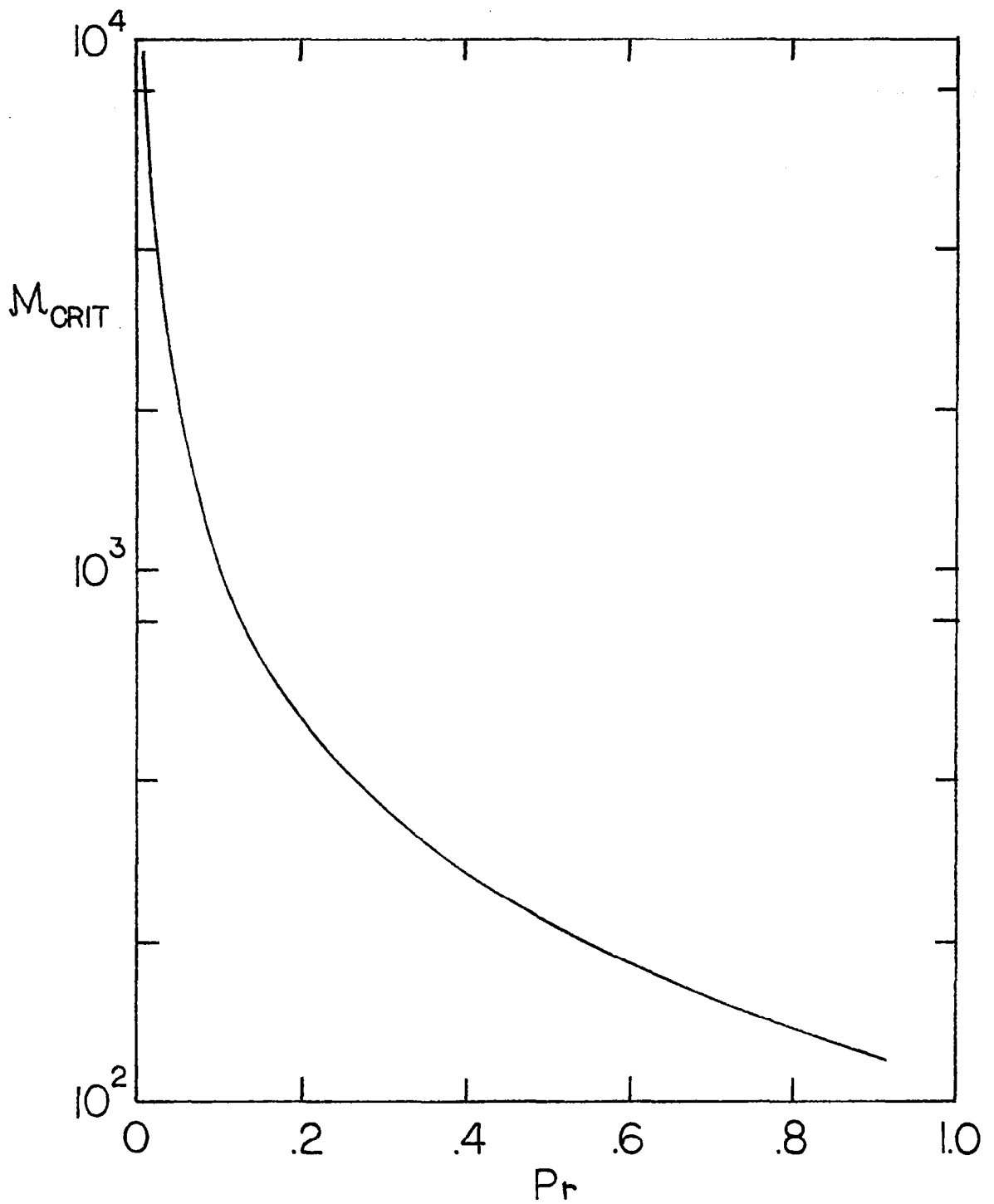


Figure 13. Variation of M_{crit} with Pr for $R = 1.0$ for the constant rate process. $Q = 1.0$, $K = 0.7$, $P = 1.0$, $C = 1.0$, $B = 1.0$. $M = R Pr M$.

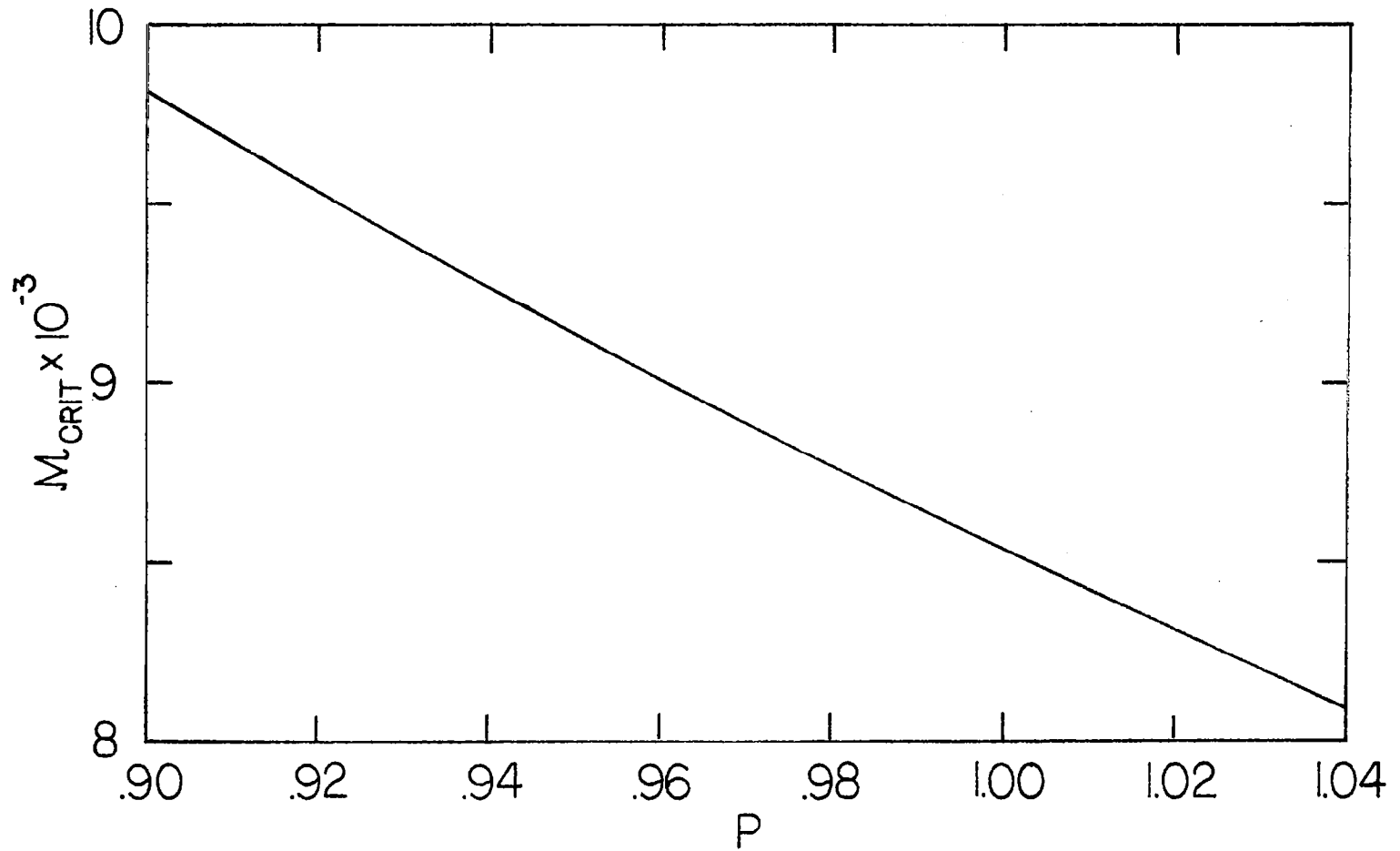


Figure 14. Effect of density change upon M_{crit} for the constant rate process. $P_r = 0.01$, $\Lambda = 175$, $Q = 1.0$, $K = 0.7$, $B = 1.0$, $R = 1.1$.

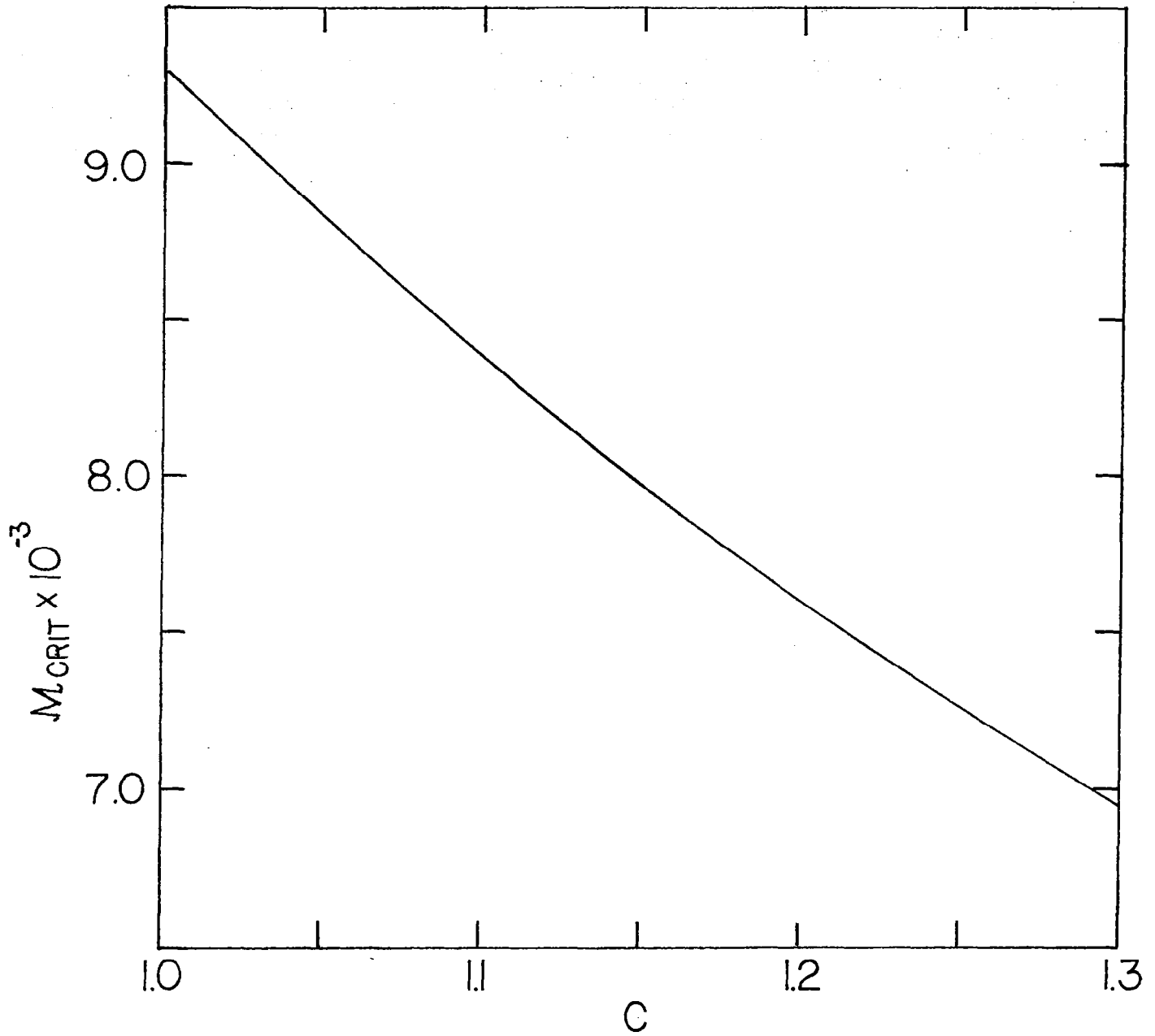


Figure 15. Effect of specific heat ratio on M_{crit} for the constant rate process.
 $P_r = 0.02$, $\Lambda = 175$, $Q = 1.0$, $K = 0.5$,
 $P = 1.0$, $B = 1.0$.

TABLE I. PROPERTIES OF MATERIALS

a) Properties of Liquid State

Material	Density (g/cm ³)	Specific heat ($\frac{\text{joules}}{\text{g}^\circ\text{C}}$)	Dynamic viscosity (g/cm sec ^{°C})	Kinematic viscosity (cm ² /sec)	Thermal conductivity ($\frac{\text{joules}}{\text{sec cm}^\circ\text{C}}$)	Thermal diffusivity (cm ² /sec)	Temperature at which properties given (°C)	Melting Temperature (°C)	Ref.
Sodium	0.928	1.378	6.80×10^{-3}	7.34×10^{-3}	0.869	0.680	97.82	97.82	a
Potassium	0.828	0.814	5.67×10^{-3}	6.85×10^{-3}	0.541	0.802	63.2	63.2	a
Bismuth	10.09	0.150	1.66×10^{-2}	1.64×10^{-3}	0.146	0.096	304	271	b
Lead	10.51	0.147	2.12×10^{-2}	2.01×10^{-3}	0.151	0.098	400	327.4	b
Tin	6.98	0.255	1.91×10^{-2}	2.74×10^{-3}	0.304	0.171	240	231.9	b
Zinc	6.92	0.501	3.17×10^{-2}	4.58×10^{-3}	0.577	0.166	500	419.5	b
Water	0.9998	4.218	1.79×10^{-2}	1.79×10^{-2}	5.66×10^{-3}	1.32×10^{-3}	0.0	0.0	c

b) Properties of Solid State

Material	Density (g/cm ³)	Specific heat ($\frac{\text{joules}}{\text{g}^\circ\text{C}}$)	Thermal conductivity ($\frac{\text{joules}}{\text{sec cm}^\circ\text{C}}$)	Thermal diffusivity (cm ² /sec)	Temperature at which properties given (°C)	Latent heat (joules/gm)	Reference
Sodium	0.951	1.361	1.191	0.914	97.82	113.2	a
Potassium	0.849	0.806	1.057	2.45	63.2	59.3	a
Bismuth	9.76	0.125	0.084	0.069	25	50.2	c
Lead	11.34	0.142	0.346	0.215	25	24.6	c
Tin	7.16	0.226	0.640	0.396	25	21.1	c
Zinc	7.40	0.389	1.150	0.400	25	102.1	c
Water	0.917	2.100	2.21×10^{-2}	1.24×10^{-2}	0.0	333.5	c

52

- References: a) Foust, O. J., editor, Sodium-NaK Engineering Handbook, Volume 1, Sodium Chemistry and Physical Properties, Gordon and Breach (1972).
 b) Ukanawa, Anthony O., "Diffusion in Liquid Metal Systems," NASA Contractor Report, Contract NAS8-30252, June 1975.
 c) Handbook of Chemistry and Physics, 54th edition, CRC Press (1973).

Table II

VALUES OF NON-DIMENSIONAL PARAMETERS

Material	$P_T(@T)^1$	Λ	K^2	Δ^2	P^2	C^2
Sodium	0.0107(100)	$83.1/\Delta T^1$	0.730	1.344	0.975	1.012
Potassium	0.0085(100)	$73.5/\Delta T$	0.511	3.050	0.975	1.011
Bismuth	0.0171(300)	$400/\Delta T$	1.74	0.715	1.034	1.20
Lead	0.0206(400)	$174/\Delta T$	0.437	2.20	0.965	1.038
Tin	0.016(240)	$93/\Delta T$	0.476	2.32	0.975	1.13
Zinc	0.0275(450)	$262/\Delta T$	0.502	2.41	0.935	1.29
Water	13.6(0)	$159/\Delta T$	0.255	9.41	1.090	2.008

Notes: 1. Temperatures measured in °C.

2. Properties determined at T_m^* for sodium and potassium and at 25°C for the solid phase for other materials.

Table III

EFFECT OF Λ ON CRITICAL MARANGONI NUMBERS
FOR STEADY STATE PROCESS

$$B=2.0, \gamma=1.2, \Delta=1.5, K=0.7$$

<u>Λ</u>	<u>Mcrit</u>	<u>$\alpha(\text{Mcrit})$</u>
2	142.6	2.3
20	150.0	2.4
200	150.6	2.4

TABLE IV

Effect of Λ on Critical Marangoni Number
for the Constant Rate Process

A. Effect of Change of L/C_{pS} .

$Pr=0.01$; $K=0.7$; $Q=2.0$; $P=1.0$; $C=1.0$; $B=1.0$.

Λ	R	M_{crit}	$\alpha(M_{crit})$
20	14.0	3.26×10^2	2.1
35	8.2	6.40×10^2	2.1
70	4.2	1.61×10^3	2.1
105	2.8	2.76×10^3	2.1
175	1.7	5.27×10^3	2.2

B. Effect of Change of $(T_2^* - T_m^*)$.

$Pr=0.01$; $K=0.7$; $P=1.0$; $C=1.0$; $B=1.0$.

Λ	Q	R	M_{crit}	$\alpha(M_{crit})$
17.5	0.5	8.4	6.22×10^2	2.1
35	1.0	5.6	1.08×10^3	2.1
70	2.0	4.2	1.61×10^3	2.1
105	3.0	3.7	1.90×10^3	2.1
175	5.0	3.1	2.18×10^3	2.1

TABLE V

Effect of Pr on Stability for R=1.0
 Q=1.0; B=1.0; K=1.0; P=1.0; C=1.0

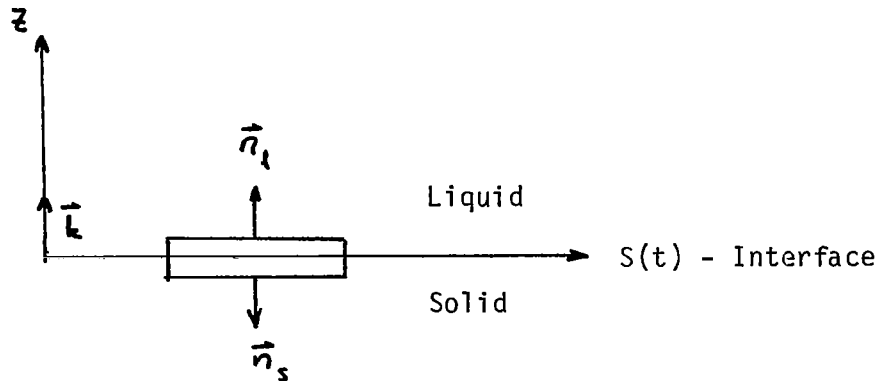
<u>Pr</u>	<u>Λ</u>	<u>M_{crit}</u>	<u>Mcrit</u>	<u>$\alpha(M_{crit})$</u>
0.002	1000	4.96×10^4	99.2	2.2
0.01	200	9.96×10^3	99.6	2.2
0.1	20	1.05×10^3	101.8	2.2
0.3	6.0	3.59×10^2	107.7	2.2
0.6	2.7	2.00×10^2	120.0	2.1
0.9	1.5	1.45×10^2	130.5	1.9

APPENDIX I

Matching Conditions

It is necessary to determine the conditions at the liquid-solid interface for arbitrary movement of that interface. Once the general relations have been derived the conditions will be linearized by assuming that the interface motion consists of a mean motion that is one-dimensional plus a small perturbation to the mean motion. The interface matching conditions will be written for a fixed laboratory frame of reference.

General interface conditions, which are expressions of the conservation of mass, momentum, and energy, are stated for a multi-component system by Williams (1965). These expressions can be specialized for a control volume consisting of a thin slab that surrounds the interface. Assuming one-dimensional mean motion the slab control volume in a fixed coordinate system is shown in the figure below.



Assume that there are no sources of mass at the surface, that the viscous stresses can be ignored, and that no chemical reactions occur. Write the velocities as follows:

$$\vec{u}_s = 0; \vec{u}_\ell = w_\ell \vec{k}; \frac{d\vec{S}}{dt} = v_p \vec{k}$$

where $\frac{d\vec{S}}{dt}$ is the velocity of the control volume and \vec{k} is a unit vector in the z direction.

The continuity equation, for this control volume [Williams, p. 14], can be written

$$\rho_\ell \left(\vec{u}_\ell - \frac{d\vec{S}}{dt} \right) \cdot \vec{k} = \rho_s \left(- \frac{d\vec{S}}{dt} \right) \cdot \vec{k}$$

or

$$\rho_\ell (v_p - w_\ell) = \rho_s v_p$$

The energy equation is

$$\left[\rho_\ell \left(e_\ell + \frac{w_\ell^2}{2} \right) \left(\vec{u}_\ell - \frac{d\vec{S}}{dt} \right) + q_\ell - p_\ell \vec{u}_\ell \right] \cdot \vec{k} = \left[\rho_s e_s \left(- \frac{d\vec{S}}{dt} \right) + q_s \right] \cdot \vec{k}$$

where

$$\vec{q} = -k \frac{dT}{dz}$$

e = specific internal energy

The momentum equation becomes

$$\rho_\ell w_\ell (w_\ell - v_p) - p_\ell = 0$$

Using this result and the continuity equation, the energy equation can be written as

$$k_s \frac{dT_s}{dz} - k_\ell \frac{dT_\ell}{dz} = \rho_s (e_\ell - e_s) \frac{dS}{dt} - \rho_\ell \frac{w_\ell^2}{2} (v_p - w_\ell)$$

But $L = e_\ell - e_s$ and the last term can be dropped because it is several orders of magnitude smaller than the other terms. Thus, we get the

following equation that was used in the solution of the mean state for both problems.

$$k_s \frac{dT_s}{dz} - k_\ell \frac{dT_\ell}{dz} = \rho_s L v_p$$

For the perturbation problems it was convenient to transform to a coordinate system fixed to the phase surface, S. If z denotes the coordinate system fixed on S, then the velocity transformation is

$$w_\ell = w'_\ell + v_p$$

The continuity equation and matching equations then become

$$\begin{aligned} \rho_\ell w'_\ell &= \rho_s w'_s \\ k_s \frac{dT_s}{dz'} - k_\ell \frac{dT_\ell}{dz'} &= -\rho_\ell w'_\ell L. \end{aligned}$$

This is eq. (16) that was used in the perturbation analysis.

Appendix II

RESULTS FOR STEADY STATE PROBLEM

Λ	B	γ	Δ	K	M crit	$\alpha(M \text{ crit})$
1000	0.0	0.2	1.5	0.7	79.603	
0.5	2.0	0.2	1.5	0.7	145.7	
5.0					150.2	
25.0					150.6	
20.0	0.0	1.2	1.5	0.7	79.0	2.0
	2.0				150.0	2.4
	4.0				216.9	2.5
	6.0				282.5	2.6
2.0	2.0	1.2	1.5	0.7	142.6	2.3
200.0	2.0	1.2	1.5	0.7	150.6	2.4

Appendix III

RESULTS FOR THE CONSTANT RATE PROCESS

Pr	A	Q	K	P	C	B	R	Mcrit	$\alpha(Mcrit)$
0.002	17.5	0.50	0.7	1.0	1.0	1.0	42.0*	4.60×10^2	2.2
		0.65					46.0	4.19	2.2
		1.0					55.0	3.47	2.2
		1.5					67.4	2.81	2.2
		2.0					79.4	2.38	2.2
		2.5					90.9	2.07	2.2
		3.0					102.0	1.85	2.2
		3.5					112.8	1.67	2.2
		4.0					123.2	1.53	2.2
		4.5					133.2	1.42	2.2
		5.0					142.9	1.33	2.2
0.002	175	1.0	0.07	1.0	1.0	1.0	5.7	5.22×10^3	2.1
		1.5					7.1	3.84	2.1
		2.0					8.6	3.01	2.1
		2.5					10.0	2.46	2.1
		3.0					11.4	2.07	2.1
		3.5					12.8	1.79	2.1
		4.0					14.3	1.57	2.1
		4.5					15.7	1.40	2.1
		5.0					17.1	1.26	2.1
0.002	175	0.50	0.7	1.0	1.0	1.0	4.3	7.80×10^3	2.1
		0.65					4.7	6.84	2.1
		1.0					5.7	5.25	2.1
		1.5					7.1	3.87	2.1
		2.0					8.5	3.04	2.1
		2.5					9.9	2.49	2.1
		3.0					11.3	2.10	2.1
		3.5					12.7	1.82	2.1
		4.0					14.1	1.60	2.1
		4.5					15.4	1.43	2.1
		5.0					16.8	1.29	2.2

*R greater than 10 are in error because the linear equation was used for their determination.

Pr	Λ	Q	K	P	C	B	R	M_{crit}	$\alpha(M_{crit})$
0.002	1000	1.0	0.7	1.0	1.0	1.0	1.0	4.96×10^4	2.2
0.01	17.5	0.50	0.7	0.97	1.0	1.0	8.2	6.50×10^2	2.1
		0.50		1.00			8.4	6.28×10^2	2.1
0.01	20.0	2.0	0.7	1.0	1.0	1.0	14.0	3.29×10^2	2.1
		3.0					18.1	2.44	2.15
		4.0					21.9	1.96	2.2
		5.0					25.5	1.66	2.2
0.01	35	1.0	0.7	1.0	1.0	1.0	5.6	1.08×10^3	2.1
		2.0					8.2	6.4×10^2	2.1
0.01	70	2.0	0.7	1.0	1.0	1.0	4.2	1.61×10^3	2.1
0.01	105	2.0	0.7	1.0	1.0	1.0	2.8	2.76×10^3	2.1
		3.0					3.7	1.90	2.1
0.01	175	0.60	0.7	1.0	1.0	1.0	0.9	1.10×10^4	2.2
		0.65					0.9	1.06	2.2
		0.70					1.0	1.03	2.2
		0.90					1.1	9.05×10^3	2.2
		1.0					1.1	8.53	2.2
		1.1					1.2	8.06	2.2
		1.2					1.2	7.64	2.2
		1.5					1.4	6.57	2.2
		2.0					1.7	5.27	2.2
		2.5					2.0	4.36	2.1
		3.0					2.3	3.69	2.1
		3.5					2.5	3.17	2.1
		4.0					2.8	2.77	2.1
4.5	3.1	2.45	2.1						
5.0	3.4	2.18	2.1						
0.01	175	0.5	0.7	0.97	1.0	1.0	0.8	1.23×10^4	2.2
		1.0					1.1	8.89×10^3	2.2
		2.0					1.6	5.51	2.2
		3.0					2.2	3.87	2.1
		4.0					2.7	2.91	2.1
		5.0					3.3	2.30	2.1

Pr	Λ	Q	K	P	C	B	R	M_{crit}	$\alpha(M_{crit})$		
0.01	175	1.0	0.7	0.90	1.0	1.0	1.0	9.79×10^3	2.2		
				0.92				1.0	9.52	2.2	
				0.94				1.1	9.26	2.2	
				0.96				1.1	9.01	2.2	
				0.98				1.1	8.77	2.2	
				1.02				1.2	8.31	2.2	
				1.04				1.2	8.10	2.2	
0.01	175	1.0	0.7	1.0	1.0	0.1	1.1	6.09×10^3	2.0		
						0.3		6.65	2.0		
						0.7		7.74	2.1		
						1.0		8.53	2.2		
						3.0		1.37×10^4	2.4		
						7.0		2.35	2.6		
						10.0		3.09	2.65		
0.01	175	1.0	0.5	0.975	1.01	0.1	1.1	6.22×10^3	2.0		
						0.3		6.79	2.0		
						1.0		8.71	2.2		
						3.0		1.39×10^4	2.4		
						10.0		3.15	2.7		
0.01	200	1.0	0.7	1.0	1.0	1.0	1.0	9.96×10^3	2.2		
0.02	175	1.0	0.5	1.0	1.0	1.0	1.0	0.6	9.30×10^3	2.2	
					1.01				0.6	9.20	2.2
					1.04				0.6	8.92	2.2
					1.10				0.6	8.39	2.2
					1.30				0.7	6.97	2.2
0.02	350	0.5	0.5	0.965	1.04	1.0	0.2	2.61×10^4	2.2		
		1.0						0.3	1.94	2.2	
		2.0						0.4	1.27	2.2	
		3.0						0.6	9.31×10^3	2.2	
		4.0						0.7	7.31	2.2	
		5.0						0.8	5.97	2.2	

Pr	A	Q	K	P	C	B	R	Mcrit	α (Mcrit)
0.05	175	0.5	0.7	1.0	1.0	1.0	0.2	1.32×10^4	2.2
		0.65					0.2	1.20	2.2
		1.0					0.2	9.85×10^3	2.2
		1.5					0.3	7.82	2.2
		2.0					0.3	6.48	2.2
		2.5					0.4	5.52	2.2
		3.0					0.4	4.79	2.2
		3.5					0.5	4.24	2.2
		4.0					0.6	3.79	2.2
		4.5					0.6	3.42	2.2
		5.0					0.7	3.12	2.2
0.1	20	0.5	0.7	1.0	1.0	1.0	0.7	1.43×10^3	2.2
		1.0					1.0	1.05	2.2
0.1	175	1.0	0.7	1.0	1.0	1.0	0.1	1.00×10^4	2.2
0.3	6.0	1.0	0.7	1.0	1.0	1.0	1.0	3.59×10^2	2.2
0.6	2.7	1.0	0.7	1.0	1.0	1.0	1.0	2.00×10^2	2.2
0.9	1.5	1.0	0.7	1.0	1.0	1.0	1.0	1.45×10^2	2.2
0.9	2.0	0.1	0.7	1.0	1.0	1.0	0.6	2.34×10^2	2.2
		0.5					0.7	1.97	2.2
		0.9					0.8	1.75	2.2
		1.0					0.9	1.71	2.2
		5.0					1.2	1.22	2.2
0.9	175	0.5	0.7	1.0	1.0	1.0	0.01	1.36×10^4	2.2
		1.0					0.01	1.02	2.2
		2.0					0.02	6.83×10^3	2.2
		3.0					0.03	5.14	2.2
		4.0					0.03	4.13	2.2
		5.0					0.04	3.46	2.2

Pr	A	Q	K	P	C	B	R	Mcrit	$\alpha(Mcrit)$
10	2.0	0.5	0.7	1.0	1.0	1.0	0.06	2.19×10^2	2.2
		1.0					0.07	1.94	2.2
		2.0					0.09	1.69	2.2
		3.0					0.10	1.58	2.2
		4.0					0.10	1.51	2.2
		5.0					0.11	1.46	2.2
10	175	0.5	0.7	1.0	1.0	1.0	0.00	1.36×10^4	2.2
		1.0					0.00	1.02	
		2.0					0.00	6.85×10^3	
		3.0					0.00	5.16	
		4.0					0.00	4.15	
		5.0					0.00	3.48	

1. REPORT NO. NASA CR-3051	2. GOVERNMENT ACCESSION NO.	3. RECIPIENT'S CATALOG NO.	
4. TITLE AND SUBTITLE Studies of Convection in a Solidifying System with Surface Tension at Reduced Gravity		5. REPORT DATE September 1978	6. PERFORMING ORGANIZATION CODE
		8. PERFORMING ORGANIZATION REPORT #	
7. AUTHOR(S) Basil N. Antar and Frank G. Collins		10. WORK UNIT NO. M-265	
9. PERFORMING ORGANIZATION NAME AND ADDRESS The University of Tennessee Space Institute Tullahoma, Tennessee		11. CONTRACT OR GRANT NO. NAS8-32484	
		13. TYPE OF REPORT & PERIOD COVERED Contractor	
12. SPONSORING AGENCY NAME AND ADDRESS National Aeronautics and Space Administration Washington, D. C. 20546		14. SPONSORING AGENCY CODE	
15. SUPPLEMENTARY NOTES Prepared under the technical mentorship of the Aerospace Sciences Division, Space Sciences Laboratory, NASA/Marshall Space Flight Center			
16. ABSTRACT The "low gravity" environment of Earth's orbit is being seriously considered for experimentation on the production of materials in space. Most of such materials processes inevitably involve either the solidification of melt or the melting of solids. Inherent in most fluid mechanisms with temperature gradients is convective motion. In this report a study is presented for the onset of convection in a solidifying system in an environment which is similar to that encountered in space processing. Since the study is for a "low gravity" condition, the only driving mechanism considered is that due to the variation of surface tension force at the free surface of the melt layer. Two simple solidification models are considered, one in which the solidification process enters in the perturbation system and another in which the melt is solidifying at a constant rate. The results show that the solidification process will bring about convection in the melt earlier than otherwise.			
17. KEY WORDS		18. DISTRIBUTION STATEMENT Category 34	
19. SECURITY CLASSIF. (of this report) Unclassified	20. SECURITY CLASSIF. (of this page) Unclassified	21. NO. OF PAGES 69	22. PRICE \$5.25